OAK RIDGE NATIONAL LABORATORY
operated by
UNION CARBIDE CORPORATION
NUCLEAR DIVISION
for the
U.S. ATOMIC ENERGY COMMISSION

ORNL - TM - 1295

TEMPERATURE DEPENDENCE OF THE RESPONSE OF LITHIUM-DRIFTED GERMANIUM DETECTORS TO GAMMA RAYS (THESIS)

M. M. El-Shishini
W. Zobel

Presented to the Graduate Council of the University of Tennessee in partial fulfillment of the requirements for the degree of Master of Science (by M. M. El-S.).

ORNL TM-1295

Contract No. W-7405-eng-26

Neutron Physics Division

TEMPERATURE DEPENDENCE OF THE RESPONSE OF LITHIUM-DRIFTED GERMANIUM DETECTORS TO GAMMA RAYS*

M. M. El-Shishini
and
W. Zobel

NOTE:

This Work Partially Supported By
NATIONAL AERONAUTICS AND SPACE ADMINISTRATION
Under Order R-104(1)

SEPTEMBER 1966

*Presented to the Graduate Council of the University of Tennessee in partial fulfillment of the requirements for the degree of Master of Science (by M. M. El-S.).

OAK RIDGE NATIONAL LABORATORY
Oak Ridge, Tennessee
operated by
UNION CARBIDE CORPORATION
for the
U.S. ATOMIC ENERGY COMMISSION

ABSTRACT

While it has generally been stated that lithium-drifted germanium detectors must be operated at liquid-nitrogen temperature for optimum performance, no systematic investigation to prove or disprove this statement has been reported. The closest experiment is that of Tavendale who, however, only investigated the resolution as a function of temperature for one low-energy gamma ray.

The resolution and efficiency of two lithium-drifted germanium detectors, approximately 20-mm diameter and 3-mm thickness, were studied in the temperature range from 85° to 160°K., using gamma-ray sources whose energies varied from 279 to 1332 kev.

It was found that, contrary to the results of Tavendale, the resolution of the detectors had a pronounced peak at about 105°K. The origin of this peak is not known, but is not due to changes in diode capacitance or leakage current. The efficiency of the diodes is approximately constant for each energy over the temperature range.

TABLE OF CONTENTS

LIST OF TABLES

LIST OF FIGURES

FIGURE PAGE

CHAPTER I

INTRODUCTION

In 1960, Pell[1,2] produced the first lithium-drifted (p-i-n) diodes with deep intrinsic sensitive layers, and suggested their use as detectors for high-energy electrons and gamma rays. In 1962, Freck and Wakefield[3] reported on a small lithium-drifted germanium detector that was 1.5 cm.^{2} x 1.5 mm. deep and had a 3.2 per cent resolution for the 662-keV. gamma rays from ^{137}Cs. The first high-resolution lithium-drifted germanium gamma-ray spectrometer was used by Webb and Williams[4] in 1963. Their detector was 0.5 cm.^{2} x 5 mm. deep and had a resolution of 1 per cent for the ^{137}Cs gamma rays. Shortly after this, Tavendale[5] produced germanium detectors up to 2.5 cm.^{2} in area by 8-mm. deep with resolutions of 0.62 per cent at 662 keV.

The potentialities of the lithium-drifted germanium gamma-ray detectors have been demonstrated and discussed by Ewan and Tavendale.[6-12] Since the detector efficiency increases with sensitive volume, and higher efficiencies are desirable for many applications, scientists are working actively on increasing the sensitive volume without degrading the resolution of the detector. As a good step toward this goal, Tavendale[12] has produced a lithium-drifted germanium detector with 16-cm.^{3} sensitive volume using the "coaxial drift technique" instead of the planar drift technique.

The production of a (p-i-n) lithium-drifted diode begins with a slab of p-type material (silicon or germanium). A layer of metallic

lithium is deposited on one side of this slab, forming an n^+-type layer and thus a diode. A reverse bias is applied for a period of time at an elevated temperature. Lithium diffuses into the slab under the influence of the applied field, producing a region of intrinsic-type material. The drift process is stopped before the compensated region extends throughout the slab, leaving a p-type layer at the back of the detector.

A diode of this type may be used as a gamma-ray detector. The gamma rays interact with the detector material by one of three types of processes: the photoelectric effect, Compton scattering, and pair production. The electrons produced in these processes cause electron hole pairs which are collected by applying an electric field across the detector. Photoelectric absorption produces a peak in the pulse-height spectrum corresponding to the full energy of the gamma ray. Compton scattering produces a continuous distribution in the pulse-height spectrum but, if the scattered gamma ray is absorbed before it can escape, the Compton event can also contribute to the full energy peak. At gamma-ray energies above 1.022 MeV., gamma-ray absorption by the pair production process becomes increasingly important. In pair production, the photon is completely absorbed and in its place appears a positron-negatron pair. In pair production, the energy spent by the pair in the crystal is equal to $E_\gamma - 2m_oC^2$ (where m_oC^2 = 0.511 MeV. is the electronic rest energy). A peak will be observed at a pulse amplitude corresponding to this energy if both annihilation quanta escape from the crystal. Those pairs for which one quantum is absorbed give rise to a peak at $E_\gamma - m_oC^2$. If both quanta are captured, a contribution to the photopeak at the full energy E_γ is obtained.

The cross section of gamma-ray absorption by the photoelectric effect, Compton scattering, and pair production is proportional to Z^5, Z, and Z^2, respectively, so a material of high Z is desirable. Hence, germanium (Z = 32) is better than silicon (Z = 14) as a gamma-ray detector. Also, the energy required to produce an electron hole pair in germanium is considerably lower than that for silicon; thus, statistical broadening will have less effect in germanium than in silicon. Further, germanium detectors have a faster rise time than silicon detectors because of their higher charge-carrier mobility. Silicon detectors have the advantage that they can be operated at room temperature in many applications, whereas germanium detectors must be operated at low temperatures. However, for high resolution applications silicon detectors must also be cooled, so this advantage is more apparent than real.

The temperature characteristics of lithium-drifted germanium gamma-ray detectors have received, as yet, little detailed experimental study. McKenzie and Bromely,[13,14] who used gold-germanium p-n junctions for the detection of charged particles in 1959, reported that germanium diodes must be operated near liquid-nitrogen temperature because, at higher temperatures, thermal generation of carriers produces excessive noise. However, they were not primarily interested in studying the temperature effect on the detector.

In 1964, Ewan and Tavendale[10] used a lithium-drifted germanium detector of 18-mm. diameter and 3.5-mm. depletion depth to study the resolution of the 122-keV. gamma-ray peak from ^{57}Co, as well as the detector leakage current, as a function of temperature at constant bias

voltage. They reported that at low temperatures the preamplifier noise is the limiting factor on resolution, and above 170°K. the detector leakage current limits the resolution. They added that the detector can be used at temperatures up to 150°K. without degradation of resolution.

Since lithium-drifted germanium detectors are coming into wider use in gamma-ray spectroscopy because of their high-energy resolution, since it is known that they must be cooled, and since comprehensive data on the temperature dependence of their response were not available, it was decided to study in detail the effect of temperature on the resolution for these detectors.

CHAPTER II

EXPERIMENTAL EQUIPMENT

A cryostat for lithium-drifted germanium gamma-ray detectors was designed and constructed such that the temperature of the diode can be varied. This is accomplished by changing the gas pressure in a vacuum jacket surrounding the diodes.

Figure 1 shows a detailed cross section of the cryostat. The canned diode is mounted on the end of a cold finger, which is a 21-in.-long hollow copper cylinder whose outer diameter is 1 in. and whose inner diameter is 0.5 in. The end opposite the diode is joined at right angles to a solid copper rod, 16.5 in. long and 1 in. in diameter. This rod is immersed in liquid nitrogen, thus cooling the detector by conduction through the hollow cylinder.

A vacuum jacket surrounds the cold finger in order to isolate it from external heat sources. This jacket is made of a 19-7/16-in.-long stainless steel cylinder which has a 2-in. outer diameter and 1.875-in. inner diameter. This shell also carries ports for mounting vacuum gauges, and connects to a gas cylinder through a palladium leak valve. The pressure within the jacket is controlled by the speed of the pumping system and the setting of this valve. The front end of the shell is closed tightly with a removable aluminum can that is 3.656 in. long and has a 1.5-in. outer diameter. The wall thickness of the can head, which faces the diode, is 0.031 in. This removable can is required to reach the diode for removal or replacement. The hollow

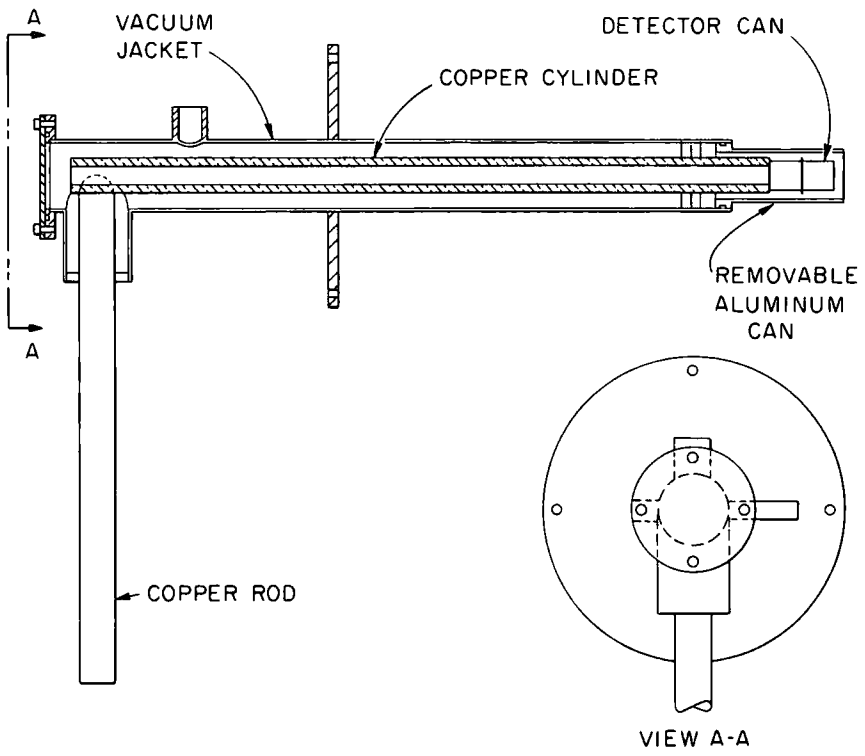

Fig. 1. A detailed cross section of the cryostat for lithium-drifted germanium gamma-ray detectors.

cylinder of the cold finger is supported in the shell by stainless steel spiders which prevent the cylinder from bending, yet minimize heat conduction from the shell to the cold finger.

The vacuum system is shown in Figure 2. It consists of a diffusion pump (CVC Consolidated Vacuum Corporation, Type VMF-11), a fore pump (W. M. Welch Manufacturing Company, Type 1402B), a cold trap, and a bleeder valve. In order to reduce pressure fluctuations inside the cryostat, the latter is evacuated through a ballast tank. The volume of this tank is approximately equal to that of the space inside the cryostat (166 $in.^3$).

An ionization vacuum gauge (Central Electronic, Type VglA/2) and a thermocouple gauge (Hasting-Raydist, Inc., Type DV-6M) are mounted on the ballast tank. The ionization gauge current is read with a Consolidated Electrodynamic Corporation, Type DPA-28 ionization vacuum gauge meter. The thermocouple gauge current is read with a Hasting Gauge, Type VT-6B.

Chromel-alumel thermocouples are used for the temperature measurements. The cold junction of such a thermocouple is soldered to a lead ring of 0.25-in. width and 0.025-in. thickness which fits tightly on the diode can. The contacting ring is made of lead since lead is a good thermal conductor and its expansion coefficient is greater than that of aluminum; hence, when the can is cooled, the lead ring shrinks faster and holds the aluminum can tightly. The thermocouple runs parallel to the hollow copper cylinder and emerges from the vacuum jacket at the end opposite the diode. The emf. induced in the thermocouple is recorded with a Minneapolis-Honeywell Multipoint Recorder.

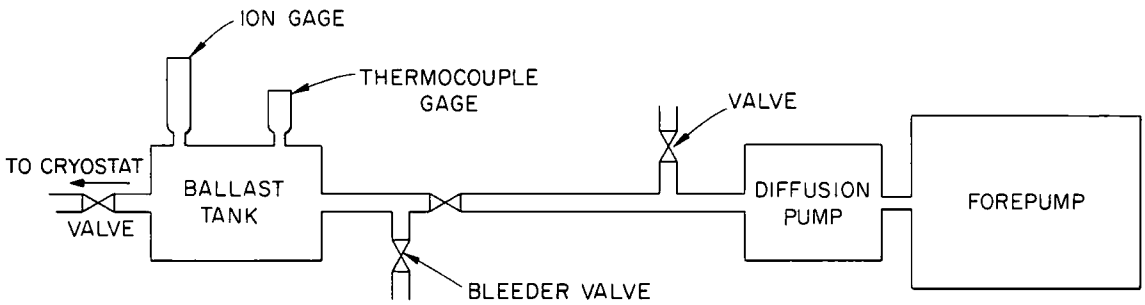

Fig. 2. The vacuum system.

Two lithium-drifted germanium diodes were used in this experiment. The two diodes are designated SG-3 and SG-1. Each diode is 19.5 mm. in diameter. The diode SG-3 has a depletion depth of 3.5 mm. and SG-1 has one of 3.0 mm. The two diodes were cut from a p-type germanium crystal which was doped with gallium and has a resistivity in the range 31-39 ohm-cm. This crystal was grown in the (1.1.1) orientation. It has a dislocation density in the range 1900-2000/cm.^{2} and a carrier life-time of 400 μsec.*

Each diode is mounted inside an aluminum can having a length of 0.78 in., an outer diameter of 0.88 in., and a wall thickness of 0.025 in. The detector is pushed against the can head by a spring which also serves as the electrical contact between the diode and an electric connector which is mounted at the center of a copper disk. This copper disk seals the diode can. It is cold welded to a lip on the can and to a similar lip on an aluminum skirt. This skirt fits tightly on the cold finger such that very good thermal contact between the diode can and the cold finger is obtained. The diode can is vacuum tight in order to avoid problems of diode surface contamination.

Detector signals are brought out of the cryostat by the use of a 0.415-in.-o.d. thin-walled stainless steel tubing coaxial line. The center conducting wire is 0.002-in.-diameter stainless steel. It is held in position by an epoxy seal at one end of the stainless steel tube

---

*Specification supplied by the manufacturer, Sylvania Electric Products, Inc.

and a glass disk at the other end facing the diode. The coaxial line is 24.5 in. long and is filled with plastic foam beads. These minimize noise that may arise from mechanical vibrations of the center wire, and prevent the line from acting as a proportional counter. At the same time the plastic has a reasonable dielectric constant so that the coaxial line still has a low capacitance (9 pf.). The coaxial line is shown in Figure 3, and a block diagram of the electronic system is shown in Figure 4.

A low-noise charge-sensitive preamplifier (Q2069C-3) designed by J. L. Blankenship[15,16] to accept and amplify the output of solid state detectors was used in the experiment. It is mounted on a flange at the end of the coaxial line. Figure 5 shows a circuit diagram of the preamplifier.

The output of the preamplifier is fed to the input of a Q2069C-1 linear amplifier, also designed by J. L. Blankenship. The amplifier chassis contains the main amplifier, a post amplifier with adjustable bias, a test pulser, and power supplies. The main amplifier is a broadband feedback-stabilized amplifier with a gain of 200 and a six-position attenuator on the input. The post amplifier has a gain of 2, 4, or 8 and includes an adjustable bias of 0 to 100 volts. The post amplifier may be switched into or out of the system. A circuit diagram of the amplifier system is shown in Figure 6.

The amplifier has two output terminals. One is connected to a single-channel analyzer and the other to a 400-channel analyzer (RIDL, Inc. Model 34-12). The single-channel analyzer is adjusted to discriminate

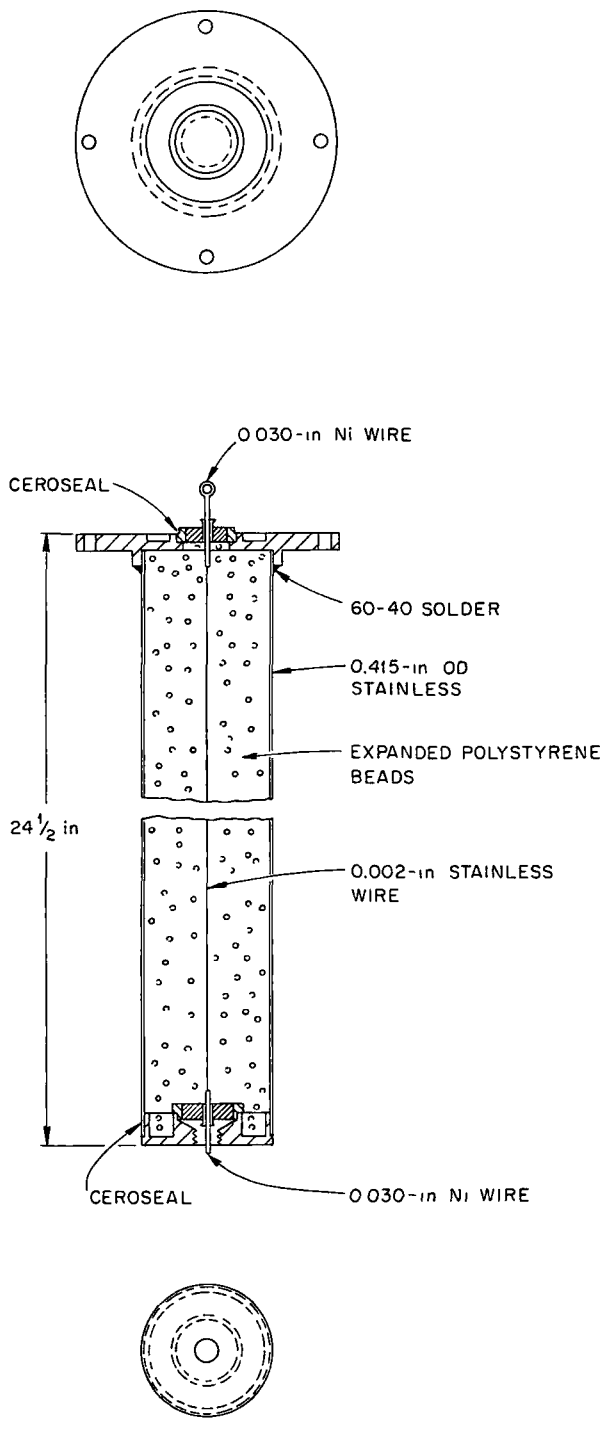

Fig. 3. The coaxial line.

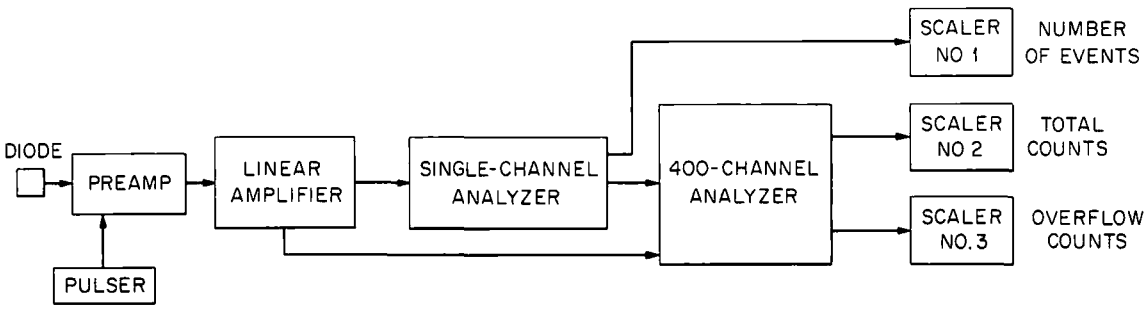

Fig. 4. A block diagram of the electronic system.

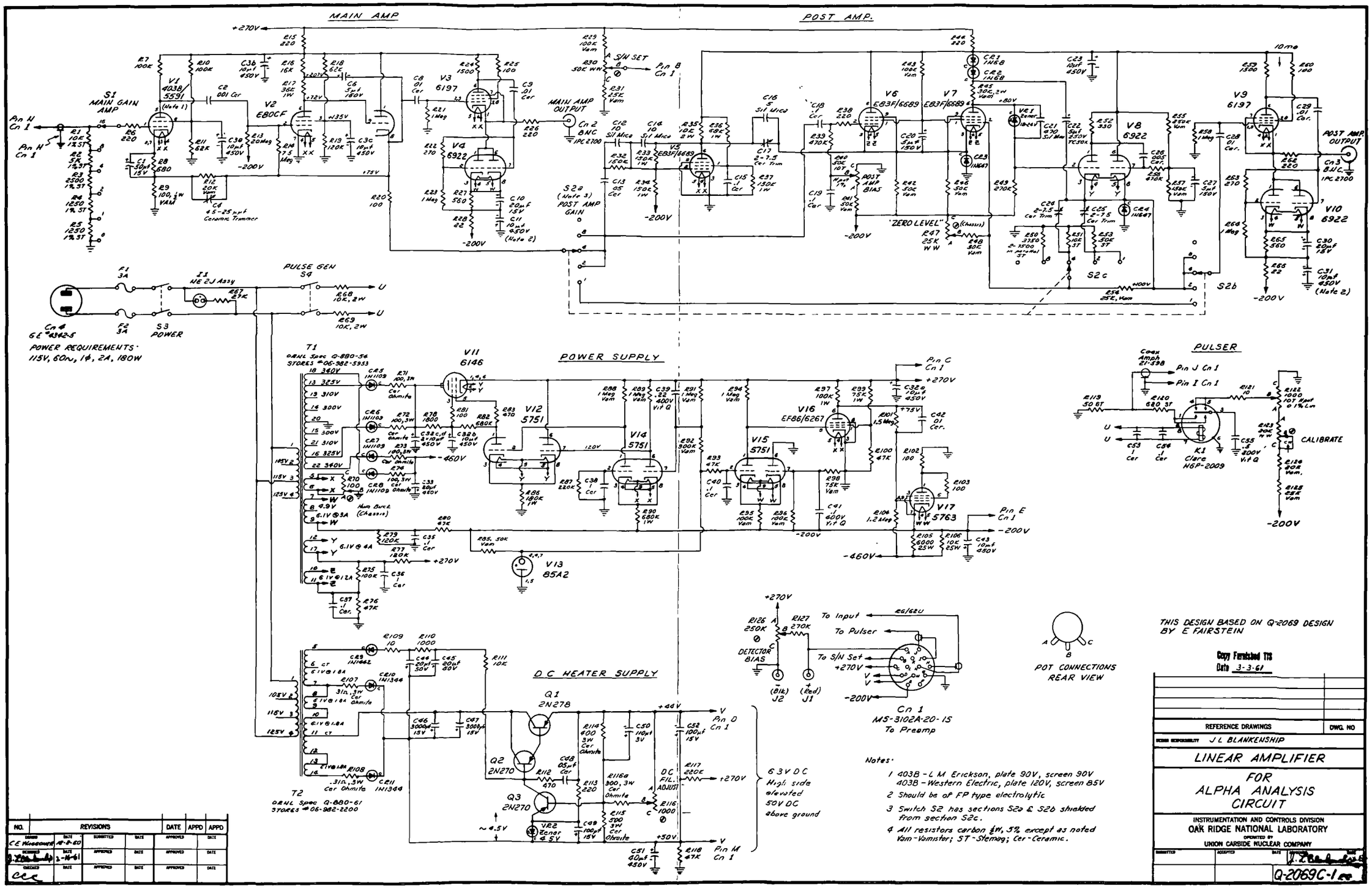

Notes:

1. 403B - L.M. Erickson, plate 90V, screen 90V
   403B - Western Electric, plate 120V, screen 85V
2. Should be of FP type electrolytic
3. Switch S2 has sections S2a & S2b shielded from section S2c.
4. All resistors carbon ½W, 5% except as noted
   Vam - Vamistor; ST - Stemag; Cer - Ceramic.

THIS DESIGN BASED ON Q-2069 DESIGN BY E FAIRSTEIN

Copy Furnished TIS
Date 3-3-61

NO.	REVISIONS	DATE	APPD	APPD
	C.E. Macdonald 12-16-60			
	2-16-61			

REFERENCE DRAWINGS — DWG. NO

DESIGN RESPONSIBILITY J.L. BLANKENSHIP

LINEAR AMPLIFIER FOR ALPHA ANALYSIS CIRCUIT

INSTRUMENTATION AND CONTROLS DIVISION
OAK RIDGE NATIONAL LABORATORY
OPERATED BY
UNION CARBIDE NUCLEAR COMPANY

Q-2069C-1

Fig. 6. The circuit diagram of the (Q2069C-1) amplifier.

14-1

14-2

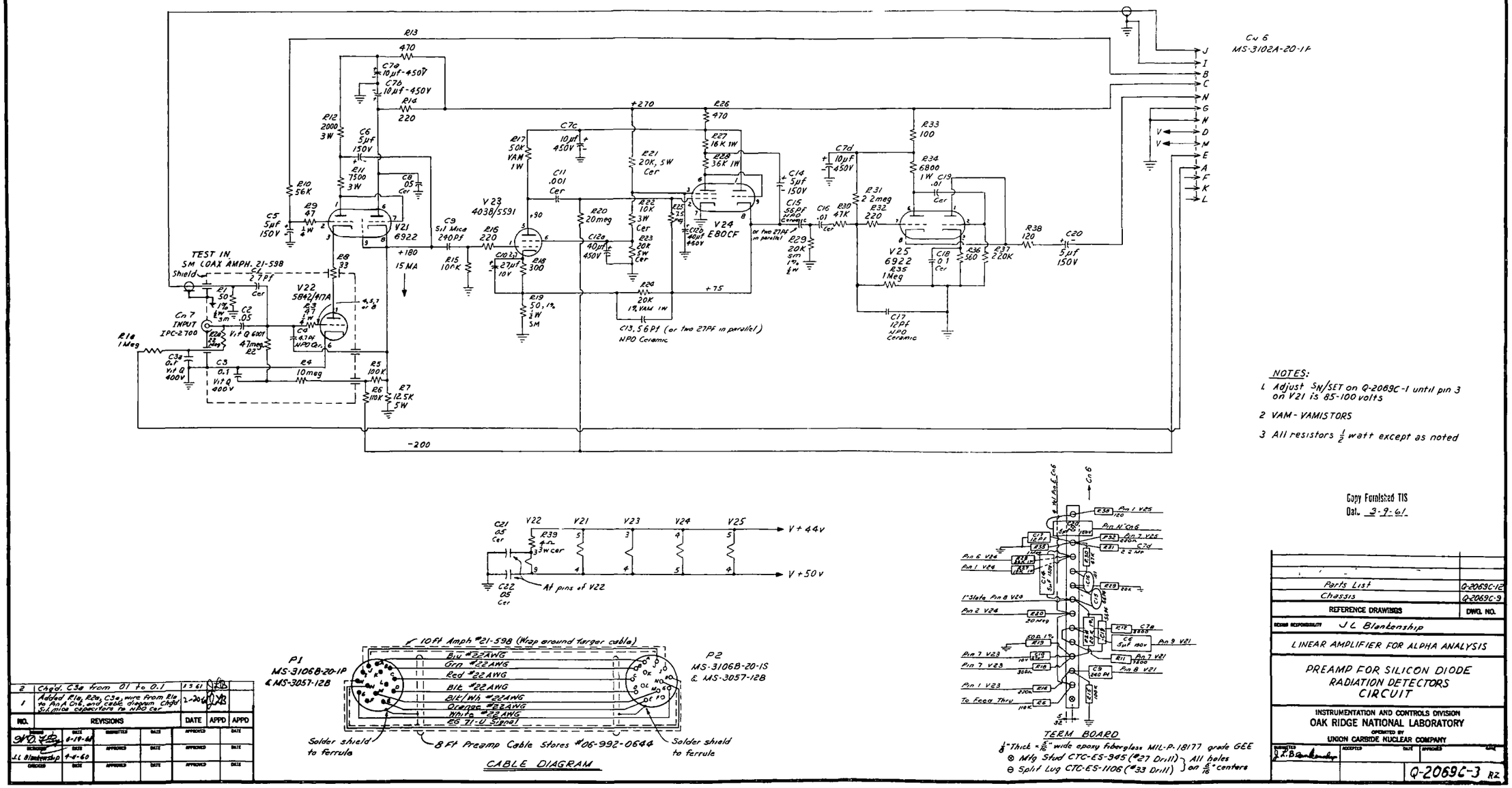

Fig. 5. The circuit diagram of the (Q2069C-3) preamplifier.

against electrical noise. The 400-channel analyzer is triggered by the output pulses of the single-channel analyzer. The 400-channel analyzer input, address overflow, and stored pulses are counted with scalers (Computer Measurements Company, Model 121FA-6462 scalers).

The diode bias voltage is furnished by a stabilized power supply (John Fluke Manufacturing Company, Inc., Model 40F).

CHAPTER III

TEMPERATURE CONTROL AND MEASUREMENTS

Two chromel-alumel thermocouples designated A and B were calibrated against a standard platinum resistance thermometer. Calibration points between 273°K. and liquid-nitrogen temperature (77.3°K.) were taken. These calibration points are given in Table 1. The accuracy of calibration is within ±0.05°K.

After the thermocouple had been calibrated at a number of points, the next requirement was a convenient means of obtaining corresponding values of emf. and temperature at other points. The wide separation of the last two calibration points (170.58°K. and 77.3°K.) makes interpolation in this range subject to large error. Interpolation between the calibration points is achieved more accurately by relating these points to an arbitrary reference table which closely approximates the temperature-emf relation of the couple. This method of interpolation is explained as follows:

A table prepared by the National Bureau of Standards for a standard chromel-alumel thermocouple[17] is chosen as the reference table. This table gives the thermocouple-induced emf. at different temperatures in the range from 1°K. to 280°K. in steps of one degree. For each calibration point the value of the induced emf. is translated into temperature by using the reference table. The difference between the temperature value obtained from the reference table and the one indicated by the platinum resistance thermometer is evaluated for each calibration point. This difference is

TABLE I

THE RELATION BETWEEN THE TEMPERATURE INDICATED WITH THE PLATINUM RESISTANCE THERMOMETER AND THE CORRESPONDING emf. INDUCED IN THE THERMOCOUPLES A AND B

Temperature indicated by platinum resistance thermometer °K	Induced emf. in mV.
Thermocouple A	
272.99	-0.0100
263.24	-0.3954
241.87	-1.2164
218.46	-2.0760
192.26	-2.9775
170.58	-3.6669
77.3	-5.8938
Thermocouple B	
272.99	-0.0098
263.22	-0.3960
241.89	-1.2157
218.47	-2.0747
192.25	-2.9762
170.58	-3.6652
77.3	-5.8945

plotted against the value of the thermocouple-induced emf. The maximum difference to be plotted is only a few degrees. Thus a smooth curve of the temperature difference versus emf. values can easily be plotted, and interpolated values can be obtained accurately in the following manner: For a certain value of emf. induced in the thermocouple one finds the corresponding temperature by using the reference table. From the difference curve one finds the difference between the temperature obtained from the reference table at that emf. value and the temperature which would be given by the standard platinum resistance thermometer. Now having the value of temperature from the reference table and its corresponding correction factor, one can find the value that would be indicated with the platinum resistance thermometer. The difference curves for thermocouples A and B are shown in Figures 7 and 8, respectively.

A subsidiary experiment was performed to determine the relation of the pressure in the cryostat jacket to the temperature of the detector. For this purpose the cold junction of thermocouple A is pushed to the center of a p-type germanium crystal (not a diode) which has the same dimensions as an actual detector and is canned in a similar manner. This thermocouple is held tightly at the copper disk, then passes through the disk, through the hollow copper cylinder of the cold finger, and out of the vacuum jacket. The cold junction of thermocouple B is soldered to a lead ring as described previously.

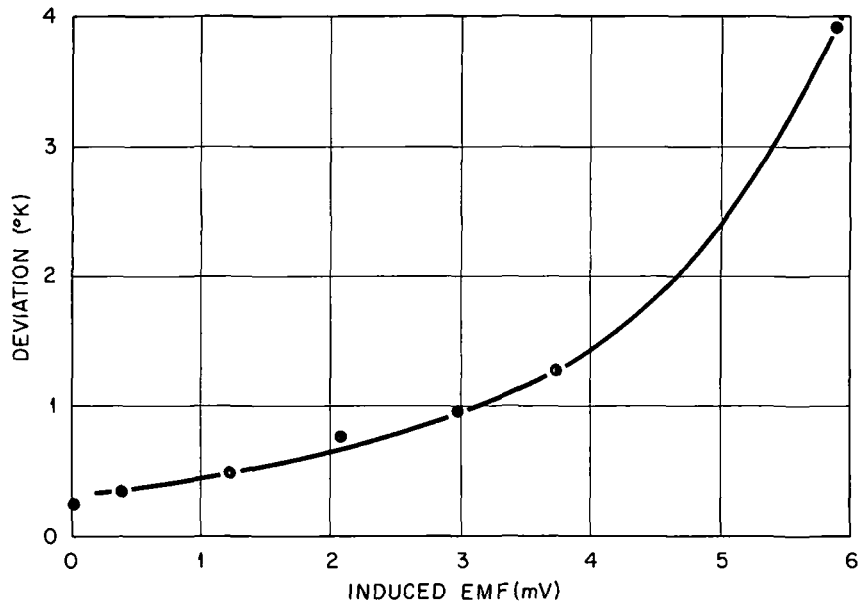

Fig. 7. The difference curve for thermocouple A.

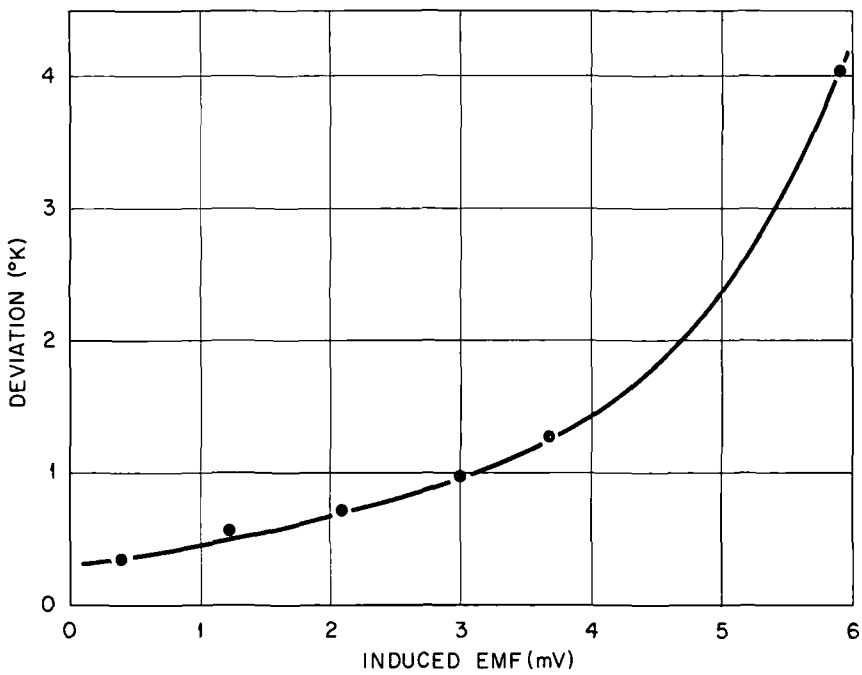

Fig. 8. The difference curve for thermocouple B.

The average length of the thermocouple wires used is 35 in. Each thermocouple is provided with chromel-alumel extension wires. Each wire of a reference junction together with a copper wire is placed in a pool of mercury at the bottom of a glass tube. The mercury forms the connection between the two wires. The glass tubes are placed in an ice bath to a depth of about 4 in. The spaces between ice particles are filled with water, thus eliminating air pockets. The ice extends all the way to the bottom of the container. The copper leads are connected to the measuring instruments.

After evacuating the system to a reasonable extent (of the order of 10^{-4} mm. mercury), the solid rod of the cold finger is immersed in a dewar filled with liquid nitrogen. When the steady state of lowest pressure and temperature is obtained, the temperature and the pressure are measured. The palladium filter is then electrically heated, thus permitting deuterium gas to flow into the system. The system pressure results from the balance between the pumping speed and the leak rate. When a steady state is again obtained, the pressure and corresponding temperature are recorded. Attainment of the steady state was assumed when the pressure and the emf. recorded by the Honeywell recorder showed no further change over a period of 20 minutes. The emf.'s of both thermocouples were displayed simultaneously on the recorder. The experiment was repeated three times. Figures 9a and 9b show the relation between the pressure inside the system and the crystal temperature obtained in the three different runs. The temperature of the crystal at a given pressure is reproducible to within $\pm 1^{\circ}K$.

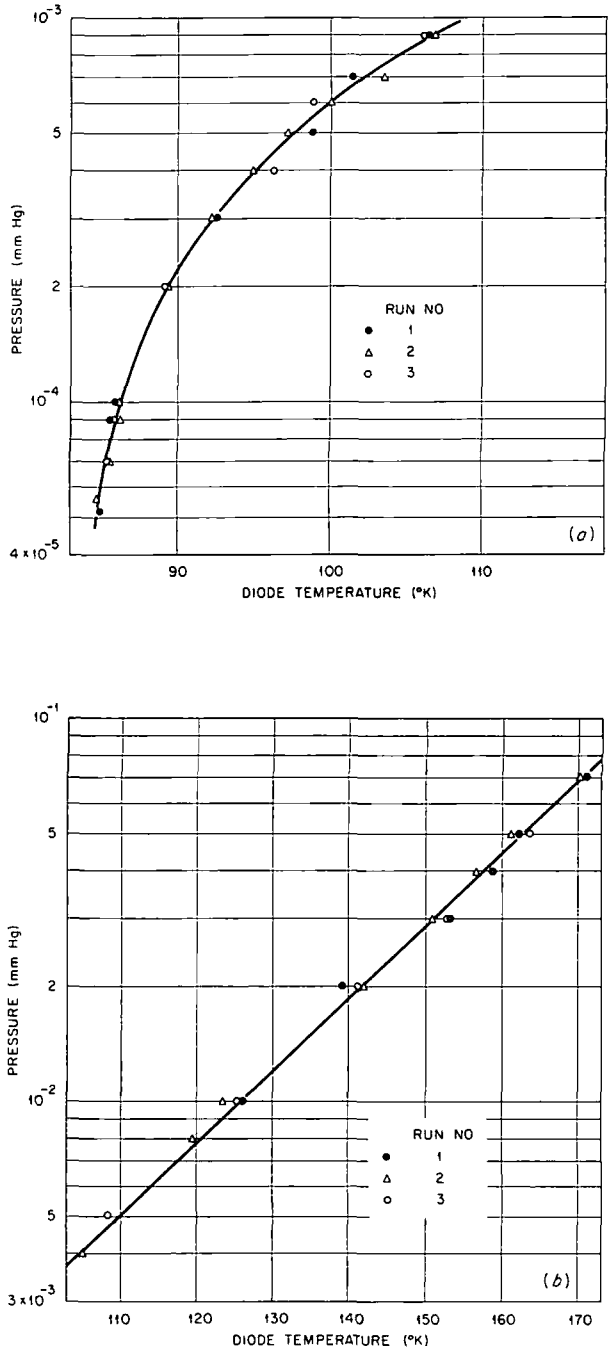

Fig. 9. The relation between the pressure inside the system and the crystal temperature. (a) lower pressure range; (b) upper pressure range.

After establishing the relation between the crystal temperature and the pressure inside the system, the dummy diode and thermocouple A are removed and an actual diode is mounted.

CHAPTER IV

EXPERIMENTAL RESULTS WITH THE DIODES

I. RESOLUTION AS FUNCTION OF BIAS VOLTAGE

Before using a semiconductor detector, it is important to determine the operating voltage at which the detector gives its best resolution. The applied bias voltage affects the resolution of the detector in two different ways:

1. The diode leakage current (which is the current that flows through the detector even in the absence of ionizing radiation) depends upon the applied bias voltage. If the applied bias voltage increases the diode leakage current will increase, thus the noise level increases and the resolution of the detector is degraded.
2. The diode bias voltage is related to the charge collection time through the approximate relation given by[18]

$$T = \frac{W^2}{\mu V}$$

where

T = charge collection time (sec.),

μ = carrier mobility ($cm^2 \cdot V.^{-1}\ sec.^{-1}$),

W = sensitive depth of detector (cm.),

V = applied voltage (volt).

Low bias voltage corresponds to a long collection time which may cause charge loss by recombination and thus degrade the resolution.

The optimum operating voltage was determined by cooling the detector to minimize the diode leakage current, maintaining it at a constant temperature, and then recording the spectrum from a simple gamma-ray source for different bias voltages. The detector energy resolution is defined as

$$\text{Energy resolution} = \frac{\text{photopeak width at half maximum height (FWHM)}}{\text{pulse height at photopeak maximum}} \times 100 \quad .$$

For a given gamma ray, the detector resolution is proportional to the full width at half maximum, therefore the term "resolution" will be used for the full width at half maximum height (FWHM). When the resolution was plotted as a function of the diode applied bias voltage, it was possible to determine the optimum operating voltage.

The diode SG-3 was cooled to 85°K., which is the lowest obtainable temperature with the present cryostat. Then the 662-keV. gamma rays from ^{137}Cs were recorded with the detector at different bias voltages. The dependence of the resolution upon the applied bias voltage for diode SG-3 at 85°K. is shown in Figure 10. It is seen that the resolution was poor when the detector was operated at low bias voltage (≤50 volts). This is believed to be due to the incomplete charge collection. Also, the resolution was poor if the applied bias voltage was ≥200 volts, which was due to the increase of the diode leakage current at high bias voltage. A

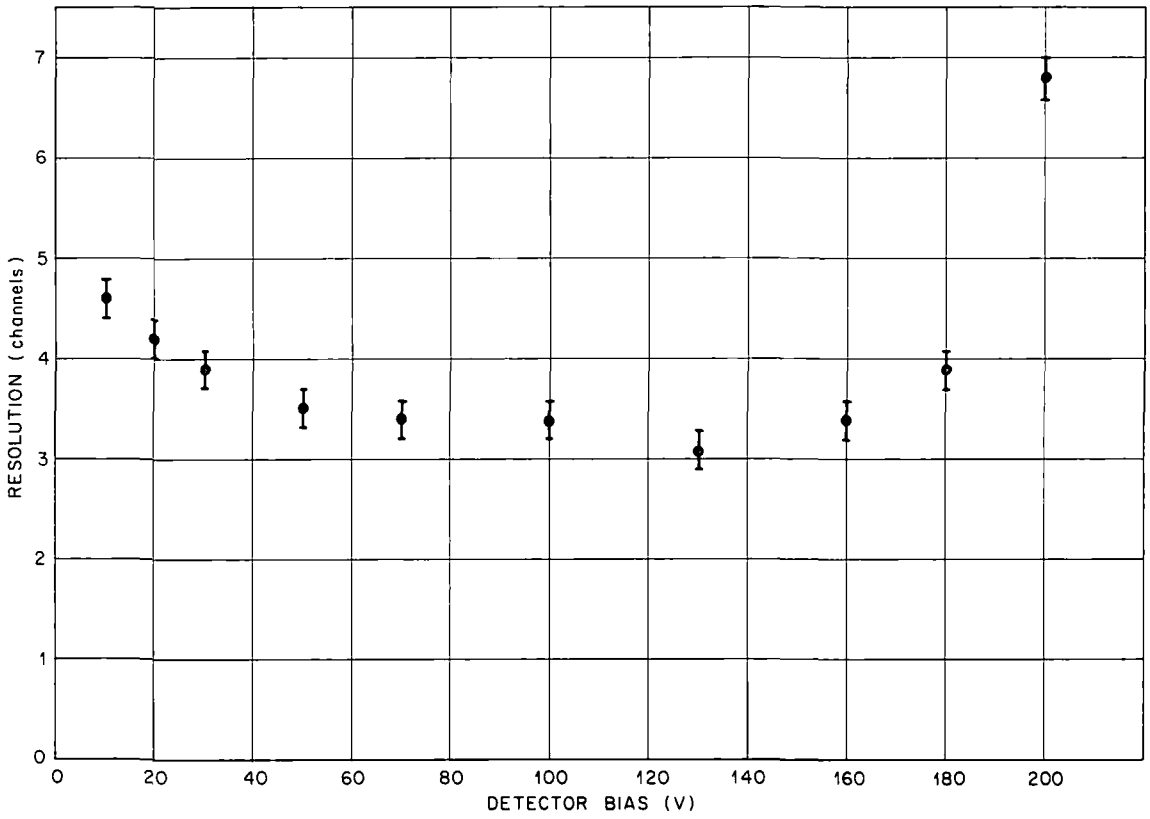

Fig. 10. Resolution of the detector SG-3 on the ^{137}Cs 662-kev. gamma-ray peak as a function of bias voltage with the detector at constant temperature ($85^{\circ}K.$).

plateau region was found in the range between 50 and 160 volts. It was therefore decided to operate this detector at 125 volts.

A similar experiment was carried out for detector SG-1 using the same gamma-ray source (^{137}Cs), but with the detector operated at two different temperatures, $85^{\circ}K.$ and $105^{\circ}K.$ As will be shown later, the detector showed a peaking in its resolution as a function of temperature at a temperature of about $105^{\circ}K.$ For this reason it was decided to study the relation between the detector resolution and its applied bias voltage at this temperature in order to see if the optimum operating bias voltage for the detector varied with temperature. The relation between the detector resolution and bias voltage at the two different temperatures is shown in Figure 11. It was found that the two curves, the one with the detector at $85^{\circ}K.$ and the other with the detector at $105^{\circ}K.$, are very similar and the plateau region does not change with temperature for this diode. It was decided to operate this detector with a bias voltage of 45 volts.

II. DIODE LEAKAGE CURRENTS

The diode leakage current is the steady current passing by the detector in the absence of radiation. It is an important factor in the operation of a detector because it can increase the electrical noise and thus limit the resolution of the detector.

The leakage current has three components:

1. The drift current due to diffusion of minority carriers into the

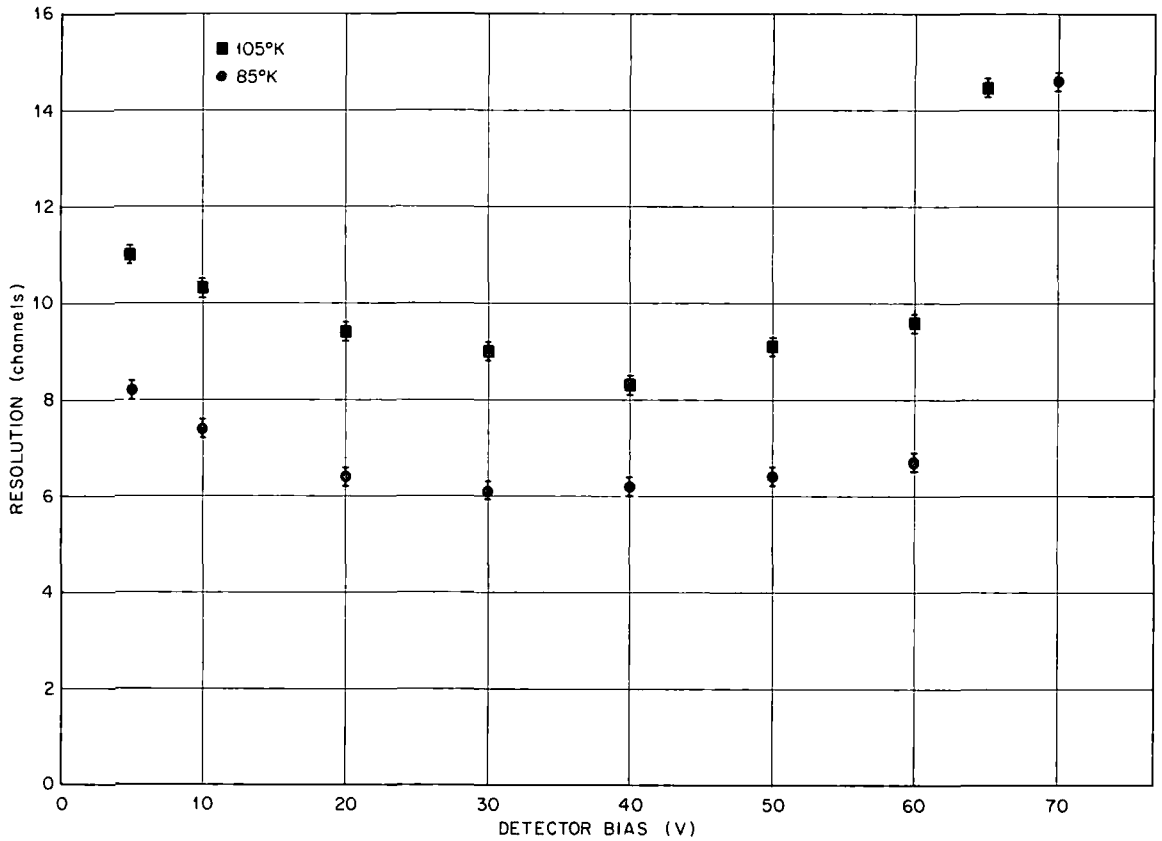

Fig. 11. Resolution of the detector SG-1 on the ^{137}Cs 662-kev. gamma-ray peak as a function of bias voltage with the detector at two temperatures (85° and $105^{\circ}K.$).

depletion zone under the influence of the electric field across the detector.

2. The carrier generation current due to carriers produced by thermal generation in the depletion layer. This depends upon the thickness of the depletion layer and the temperature of the diode. It increases with increasing temperature, and it is higher for larger depletion regions.

3. The surface leakage current, which is the current that flows through the surface layer. It depends strongly upon the nature of the surface contamination.

The drift current is very small compared with the surface and generation currents. Hence the diode leakage current can be reduced by cleaning the detector surface, thus reducing the surface current. Cooling the detector minimizes the thermal generation currents.

Since the detector leakage current changes with temperature, it was necessary to study the variation of the detector leakage current with temperature.

The diode leakage currents for both diodes SG-3 and SG-1 were measured as a function of temperature with the detectors biased at the previously chosen operating bias voltages. The leakage current was obtained by measuring the potential drop across a 12.084 ± 0.006 megohm resistor in series with the diode. A d.c. microvoltmeter, Dynamics Instrumentation Company, Model 1362, was used for these measurements. The diode leakage current was first measured while the detector was at 85°K. Then the gas pressure was adjusted at a value which corresponds

to a temperature of 95°K. After the temperature of the diode reached the steady state (which is assumed by the constant emf. recorded by the Honeywell recorder), the leakage current was measured again. Similarly, measurements were taken at 105°, 115°, 145°, and 160°K. The diode leakage current as a function of temperature for diodes SG-3 and SG-1 is shown in Figure 12. From this figure it is seen that the diode leakage current increases as the diode temperature increases.

III. DIODE CAPACITANCE

The noise of the preamplifier is strongly dependent upon the capacitance of the detector and its leads to the preamplifier. This electrical noise is superimposed on the current pulses obtained from the absorption of ionizing radiations, and causes a broadening of the pulse-height spectrum. The effect of electrical noise in a detector-amplifier system is explained by the following equation:[18]

$$(E_{FWHM})^2 = 0.75\left[2 \times 10^{-2}\frac{C^2}{g_m T} + 2 \times 10^{-4} C^2 + 1.6 \times 10^{-1} T(i_g + i_L) + \frac{8T}{R}\right] ,$$

where E_{FWHM} is the noise in terms of the full width at half maximum of a monoenergetic line in a spectrum obtained with a germanium detector (expressed in keV.), C is the total input capacity for detector and electronics (in picofarads), T is the amplifier integrator and differentiator time constant (in μsec.), $i_g + i_L$ is the sum of detector leakage and tube grid current (in nanoamperes), R is the shunt resistance in the input circuit (in megohms), and g_m is the mutual conductance of the input

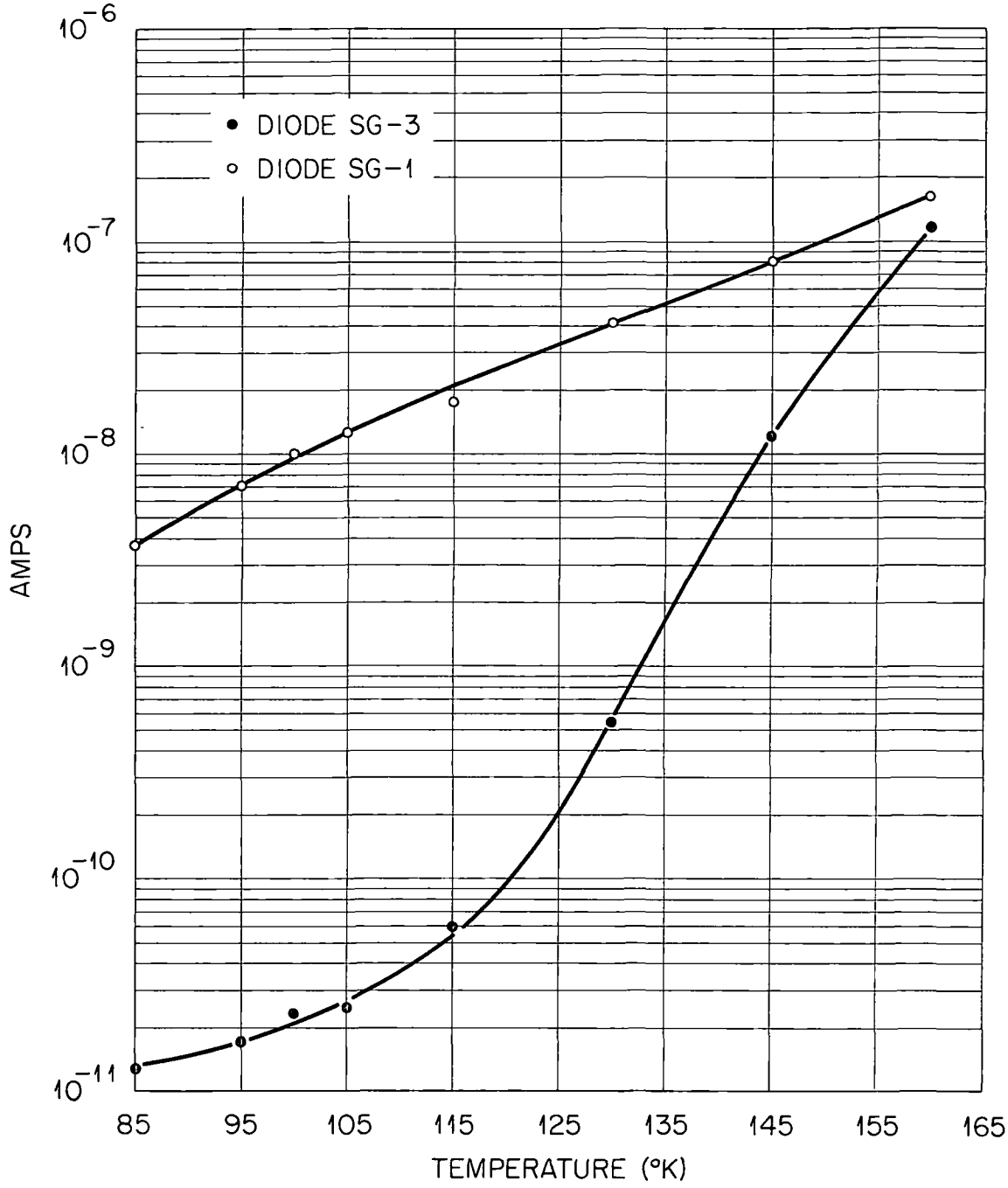

Fig. 12. Detector leakage current as function of temperature.

tube (in mA./volt). The first term of this equation is called the tube shot noise, the second the tube flicker noise, the third the current noise, and the fourth the input resistance noise.

From this equation it is obvious that the amplifier input capacitance and diode leakage current affect the resolution. For this reason the diode leakage current must be reduced by cooling the detector, and the preamplifier input capacitance must be as low as possible in order to reduce the electrical noise.

Since the capacitance of the detector and its connecting leads affects the preamplifier noise and thus the energy resolution, it is important to know its value and to see if it changes with temperature.

The diode capacitance was measured with a capacitance meter (Rohdle and Schwarz, Model Karn 510 FNRM519/81) while the diode was mounted on the cold finger and connected to the signal cable. First the zero of the capacitance meter was determined, and then the capacitance of the connecting leads and the detector attached to the coaxial cable was measured. Knowing the capacitance of the connecting leads and the coaxial cable, the detector capacitance was evaluated.

The diode SG-3 had a capacitance of (14.4 ± 1.2) pf. at 85°K. and the diode SG-1 had a capacitance of (22.0 ± 1.1) pf. at the same temperature. The diode capacitances were measured with the diodes biased with the previously determined optimum bias voltage, which is 125 volts for diode SG-3 and 45 volts for diode SG-1. The relation between the diode

capacity and its temperature is shown in Figure 13 for both diodes SG-3 and SG-1. It was found that the diode capacity does not change with temperature.

IV. GAMMA-RAY SPECTRA AT DIFFERENT TEMPERATURES

In order to study the effect of temperature on the response of lithium-drifted germanium gamma-ray detectors it is important to measure accurately both the resolution for some gamma-ray sources and the detector efficiency (which is taken as the area under the gamma-ray photopeak stored in a certain time) as a function of the detector temperature.

The gamma-ray sources used in this experiment are listed in Table II. All these sources are canned in stainless steel cylinders except ^{22}Na, which is canned in a brass cylinder. All source cans have 0.25-in. outer diameters except ^{60}Co which has a slightly larger diameter.

The canned source was pushed with a little pressure to the end of a hole drilled all the way through the center of a plexiglas cube of 2-in. side length. The source was kept at a fixed position inside the block which was put on a table whose height was adjusted such that the source center and the detector center were on the same horizontal line. The source position was marked on that table. The distance between a source and the detector was chosen such that the counting rate is about 500 counts per second in order to avoid problems of high counting rates (>1000 counts per second). These problems are mainly (1) the limited ability of the electronic system to count accurately because of its limited resolving power, and (2) the pile-up of pulses which takes place

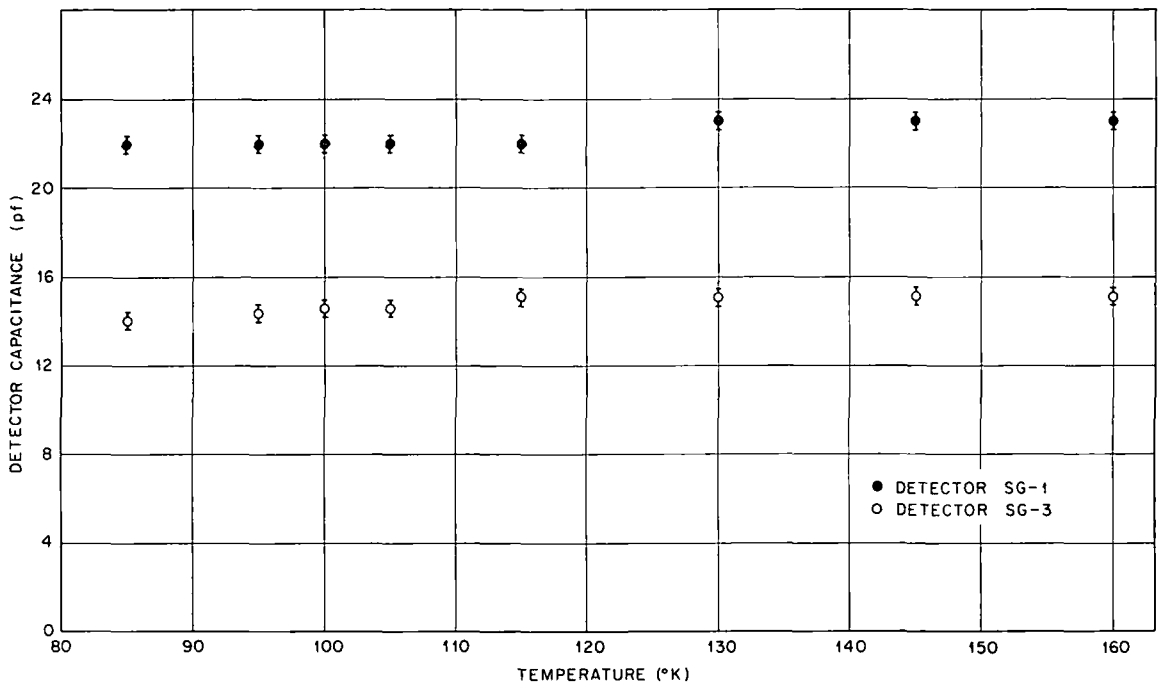

Fig. 13. Capacitance of the detectors SG-3 and SG-1 as function of temperature.

TABLE II

THE GAMMA-RAY SOURCES USED IN THE EXPERIMENT AND THEIR ENERGIES

Source	Gamma-ray energies (keV.)
^{60}Co	1332.48 ± 0.05
^{60}Co	1173.23 ± 0.04
^{22}Na	1274.6 ± 0.3
^{22}Na	511.003 ± 0.005
^{137}Cs	661.65 ± 0.1
^{113}Sn	392.6 ± 0.8
^{203}Hg	279.12 ± 0.05
^{88}Y	1836.2 ± 0.3
^{88}Y	898 ± 0.3

when more than one pulse occurs during a time interval of the order of the pulse duration, resulting in unwanted counts whose amplitudes do not represent the height of the actual pulse. Since the outer diameter of the can containing ^{60}Co was slightly greater than the diameter of the hole through the plexiglas block, the latter could not be used and this source was put directly on the table. The geometry of the cobalt source position was not as precisely reproducible throughout the experiment.

As mentioned above, it was desired to measure the spectrum from sources having gamma rays with energies as high as 1333 keV. and as low as 279 keV. In order to display all of these spectra simultaneously in a 400-channel analyzer it would be necessary to have a gain of about 3.5 keV./channel, so that the highest energy gamma ray would fall within the analyzer range (i.e., this line would be stored in channel 381). With an expected full width at half maximum of about 8-10 keV. for these gamma-ray lines, this gain implies that a peak extends over approximately five channels. Such a narrow peak does not lend itself well to accurate measurements of the peak width. It was therefore desirable to decrease the gain by at least a factor of two in order to spread the peak over more channels. It was found possible to cover the whole energy range in two segments, one covering energies below about 750 keV. and the other those above 750 keV. The gains corresponding to these ranges are 1.68 keV./channel for the lower one and 1.72 keV./channel for the upper one.

The first series of measurements was made using diode SG-3. The spectra from the sources listed in Table II were taken at 85°K., which

was the lowest temperature easily attainable with this equipment. Representative spectra are shown in Figures 14 and 15. The detector was then permitted to warm up by increasing the gas pressure in the jacket surrounding the cold finger until the temperature reached 95°K. After steady state was reached as indicated by the thermocouple attached to the detector can, the spectra from all the sources were again taken. This procedure was repeated so that all spectra were measured at the temperatures listed in Table III.

It is possible, of course, that the sequence of measurement, i.e., the monotone increase in temperature of the diode, can give rise to a systematic error. Therefore, the experiment was repeated starting at 160°K., but decreasing the diode temperature to the same values as had already been used. For this phase of the experiment only ^{22}Na and ^{113}Sn sources were used, the former being representative of the high-energy gamma rays, and the latter of the low-energy ones. The results are shown in Figure 16. It is evident that there is no systematic change in the result, whether the detector is warmed or cooled.

In removing the diode from the cold finger in preparation for the next series of measurements, the skirt on the can became detached. This made it impossible to use the diode again in this experiment because time did not permit it to be recanned. It is for this reason that certain measurements were carried out with diode SG-1 but not with diode SG-3.

The series of measurements described for diode SG-3 was repeated for diode SG-1, and representative spectra obtained at 85°K. for this diode are shown in Figures 17 and 18. Since there had been no evidence

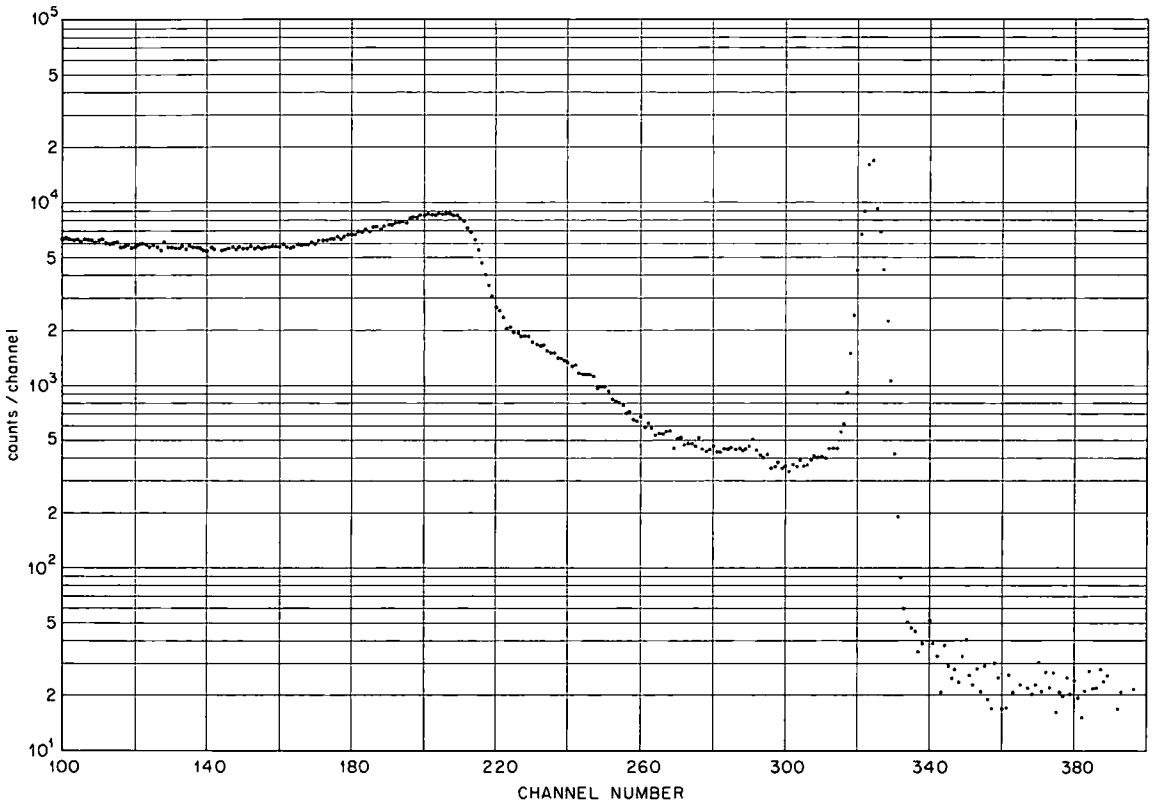

Fig. 14. Pulse-height spectrum of ^{137}Cs 662-kev. gamma-ray observed with detector SG-3 at $85^{\circ}K$.

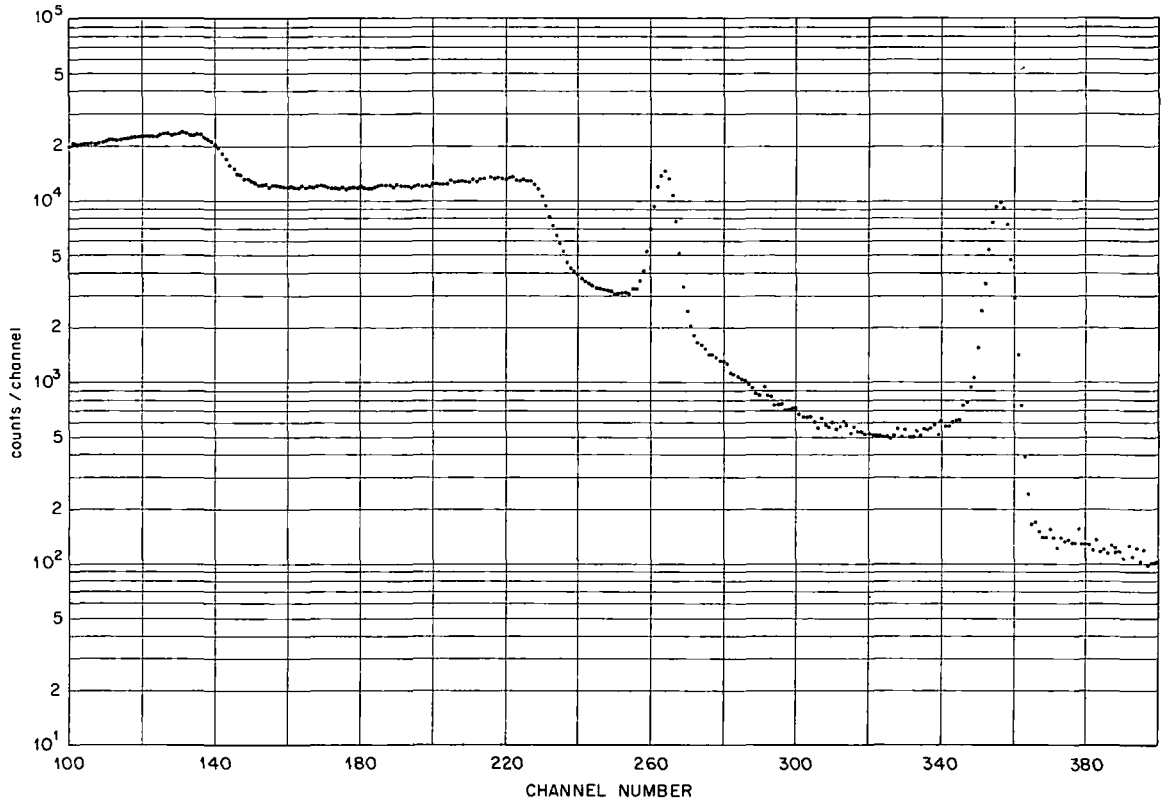

Fig. 15. Pulse-height spectrum of ^{60}Co observed with detector SG-3 at 85°K.

TABLE III

TEMPERATURES (^{o}K.) AT WHICH THE DETECTORS SG-3 AND SG-1 WERE OPERATED

Detector SG-3	Detector SG-1
85	85
95	95
105	100
115	105
130	115
145	130
160	145

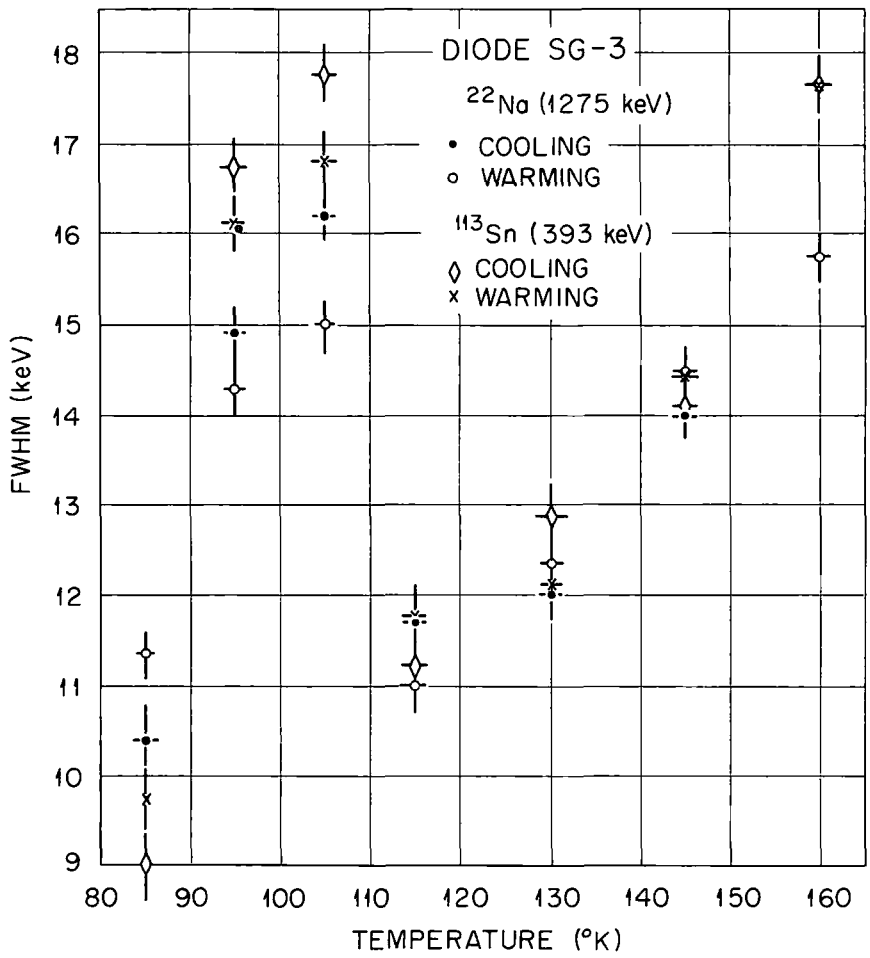

Fig. 16. Resolution of the detector SG-3 on the ^{113}Sn and ^{22}Na 1275-kev. gamma-ray peak as a function of temperature during the warming and cooling processes.

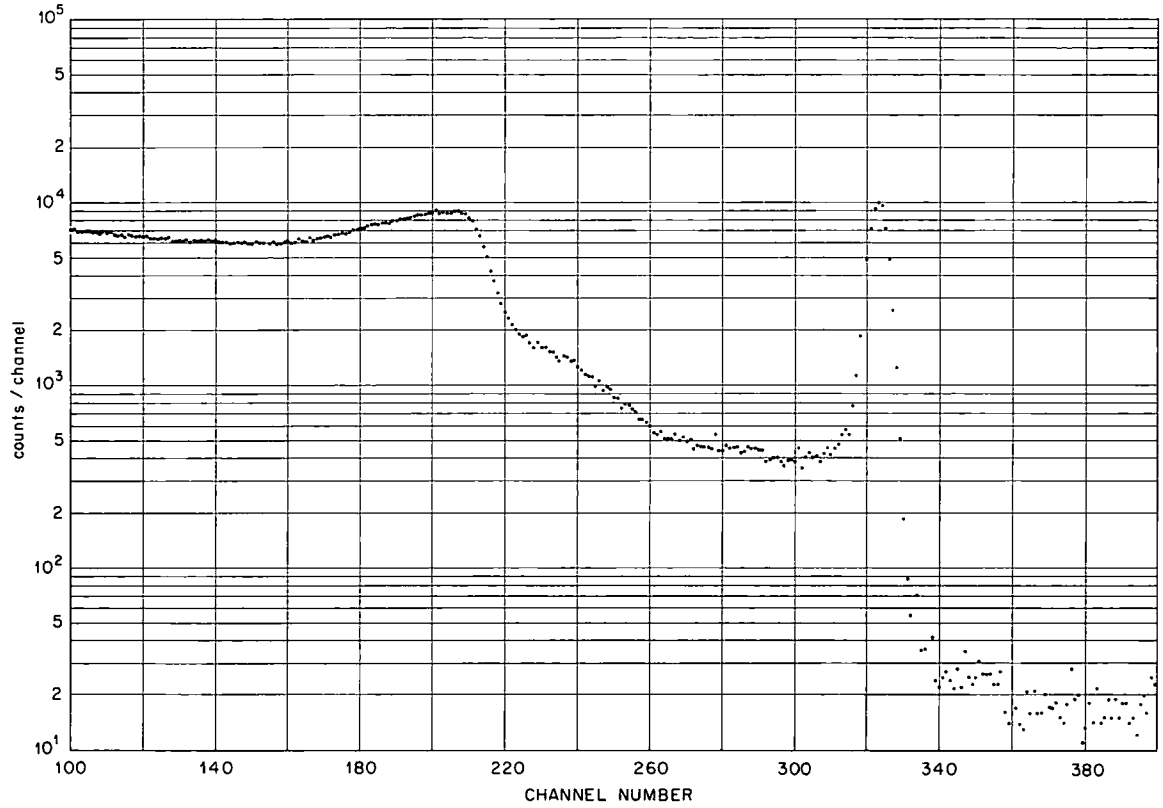

Fig. 17. Pulse-height spectrum of ^{137}Cs 662-kev. gamma ray observed with detector SG-1 at 85°K.

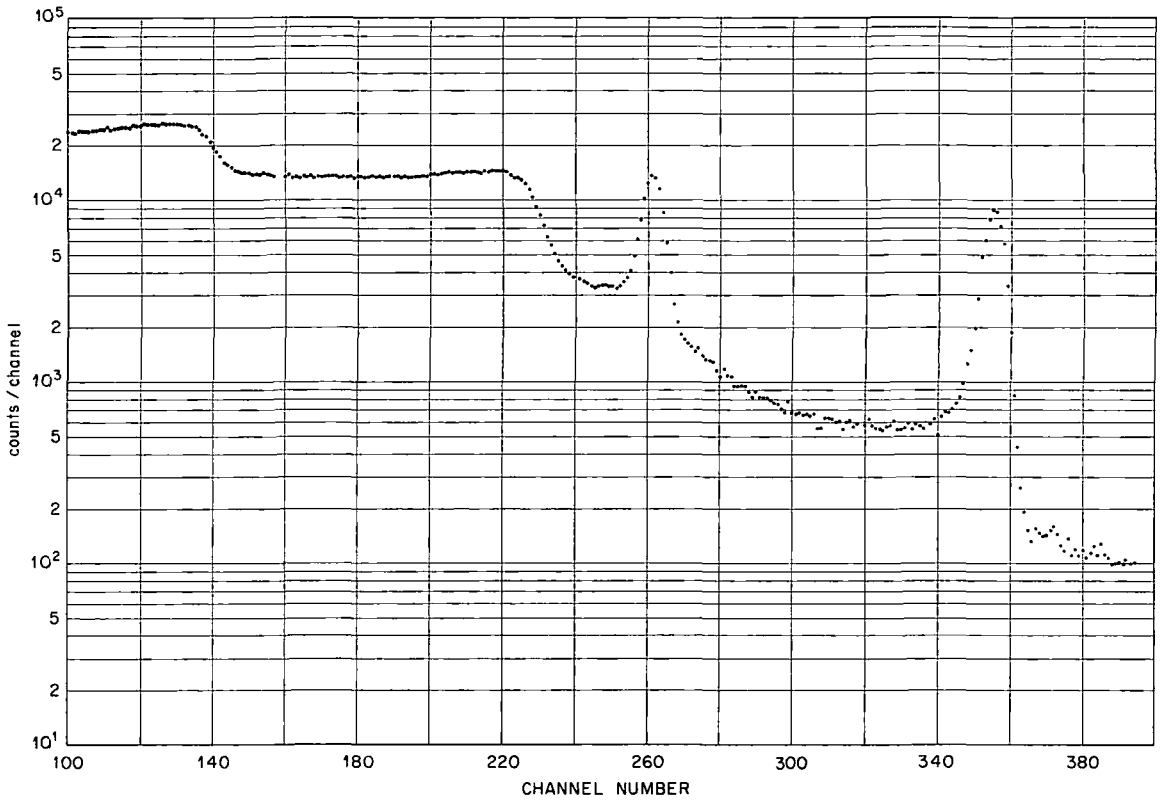

Fig. 18. Pulse-height spectrum of ^{60}Co observed with detector SG-1 at 85°K.

of a dependence of the results on the order in which the temperature of the detector was varied, the cooling sequence was eliminated from the experiment for this diode. The results from this series of measurements, together with the results from the SG-3 series, are presented in Figures 19-26.

For both diodes SG-3 and SG-1, the storing time was taken to be long enough to have a peak height of about 10,000 counts in order to reduce the statistical error.

The single escape peak corresponding to the ^{88}Y 1836.2-keV. gamma ray was not analyzed because of its low intensity, and the double escape peak was not analyzed because it differs only from the ^{88}Y 898-keV. gamma ray by 84 keV.

It was observed that for all the different gamma-ray sources used in the experiment the resolution of the two diodes showed a peak in the resolution temperature curve at a temperature of about 105°K. In order to examine the nature of this peaking, an auxiliary experiment was carried out with detector SG-1. In this experiment the resolution of the diode was studied as function of temperature using the ^{137}Cs gamma ray and a mercury pulser, which was adjusted to give pulses with height equal to that from Cs. The result is shown in Figure 27. It was found that the pulser line width which represents the amplifier noise increases continuously and slowly as the temperature increases, probably because of the increase in the diode leakage current. The line width of the gamma rays exceeds that of the pulser due to statistical variations in formation and

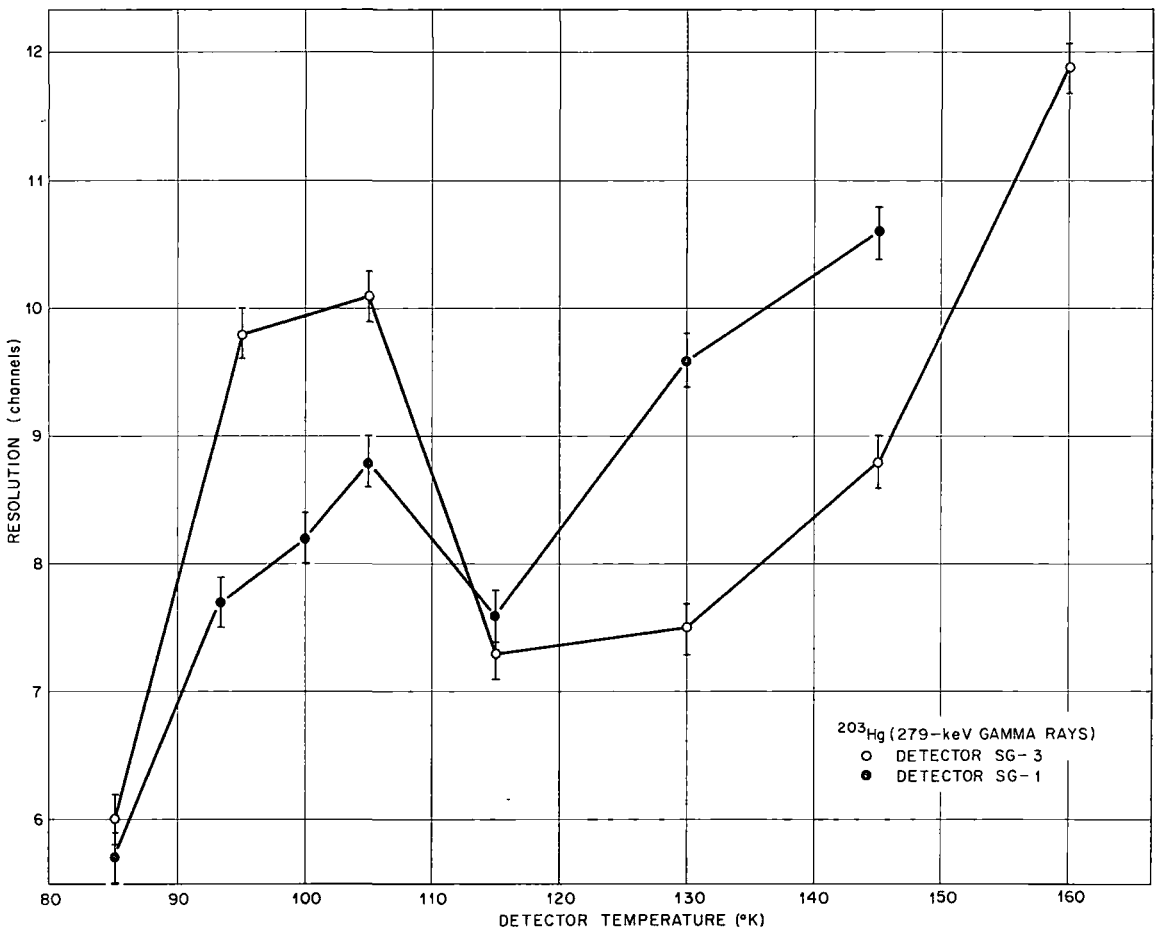

Fig. 19 Resolution of the detectors SG-3 and SG-1 on the ^{203}Hg 279-kev. gamma-ray peak as function of temperature.

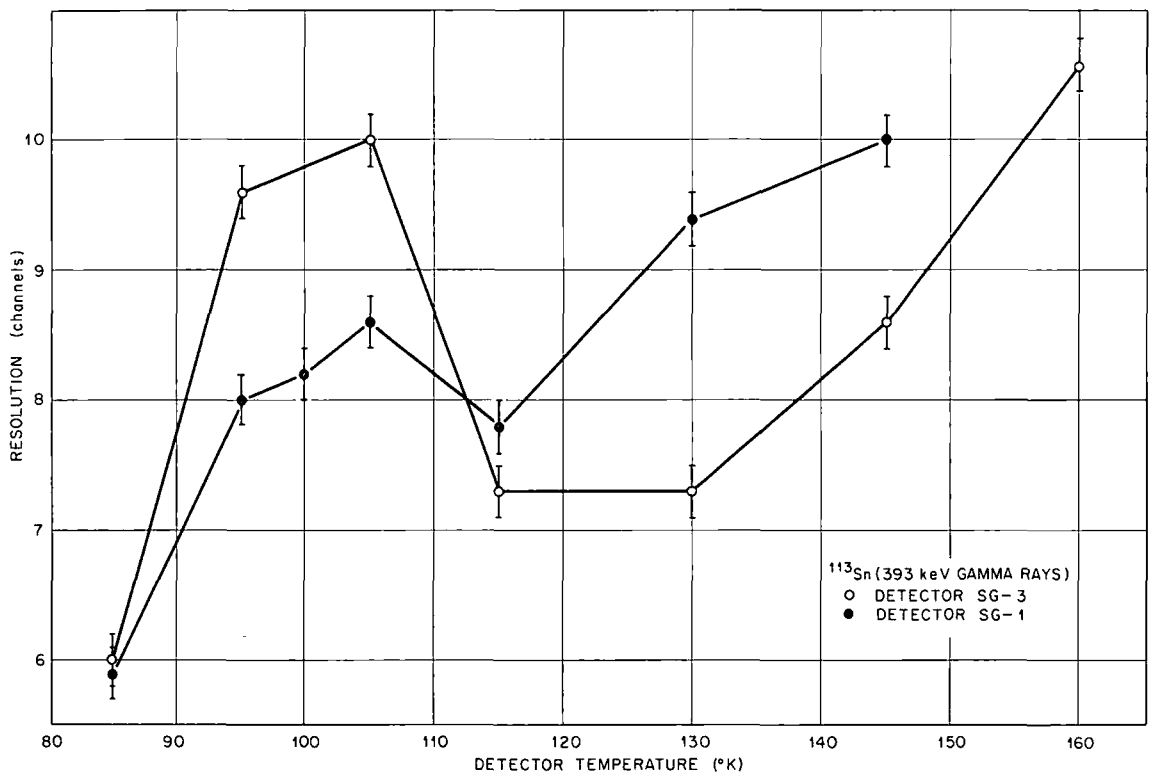

Fig. 20. Resolution of the detectors SG-3 and SG-1 on the ^{113}Sn 393-kev. gamma-ray peak as function of temperature.

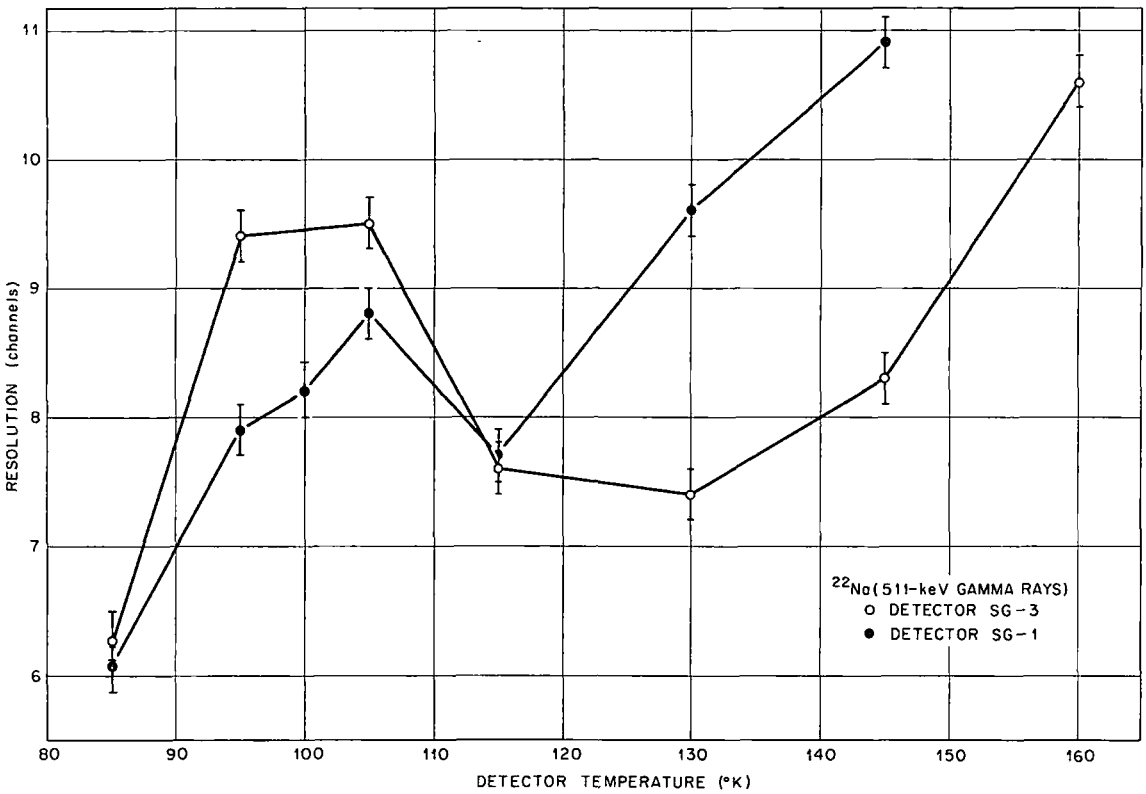

Fig. 21. Resolution of the detectors SG-3 and SG-1 on the ^{22}Na 511-kev. gamma-ray peak as function of temperature.

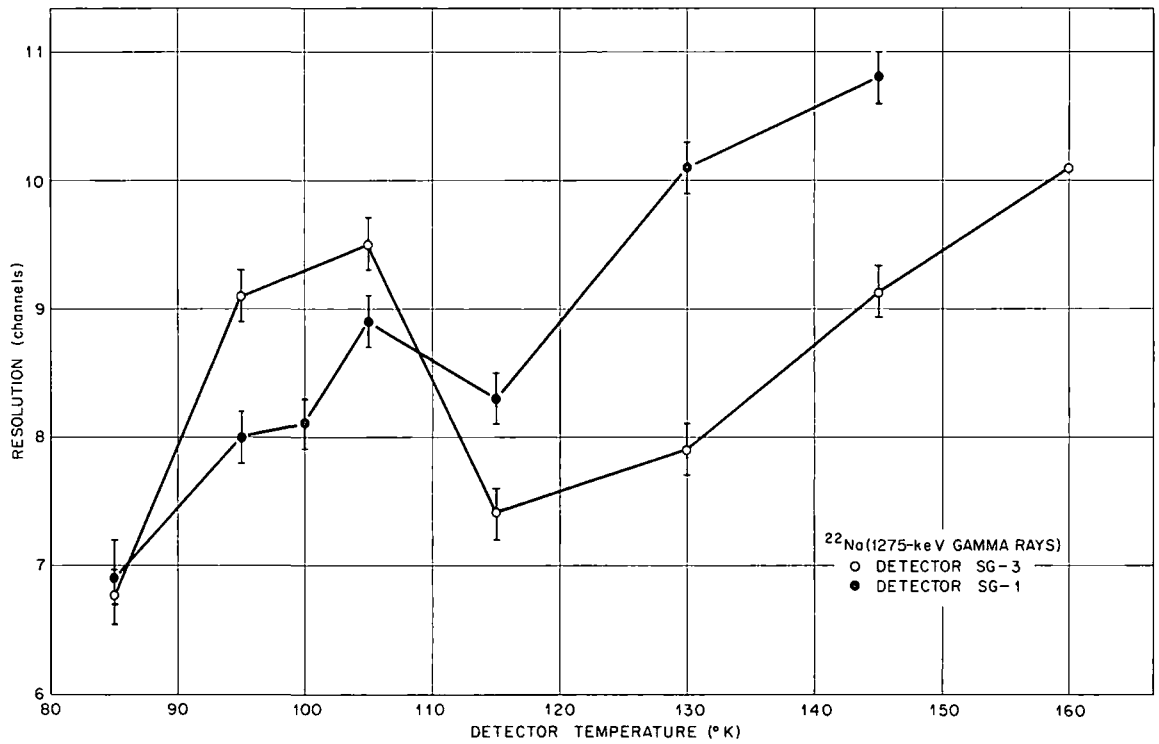

Fig. 22. Resolution of the detectors SG-3 and SG-1 on the ^{22}Na 1275-kev. gamma-ray peak as function of temperature.

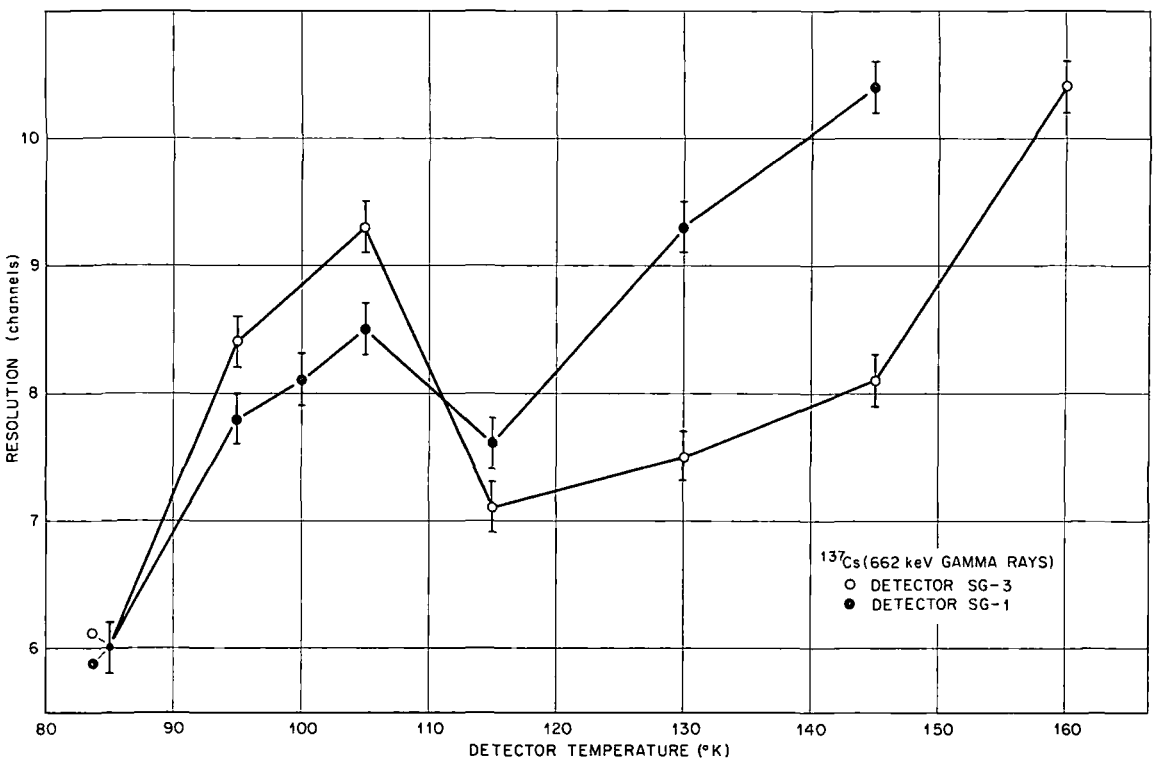

Fig. 23. Resolution of the detectors SG-3 and SG-1 on the ^{137}Cs 662-kev. gamma-ray peak as function of temperature.

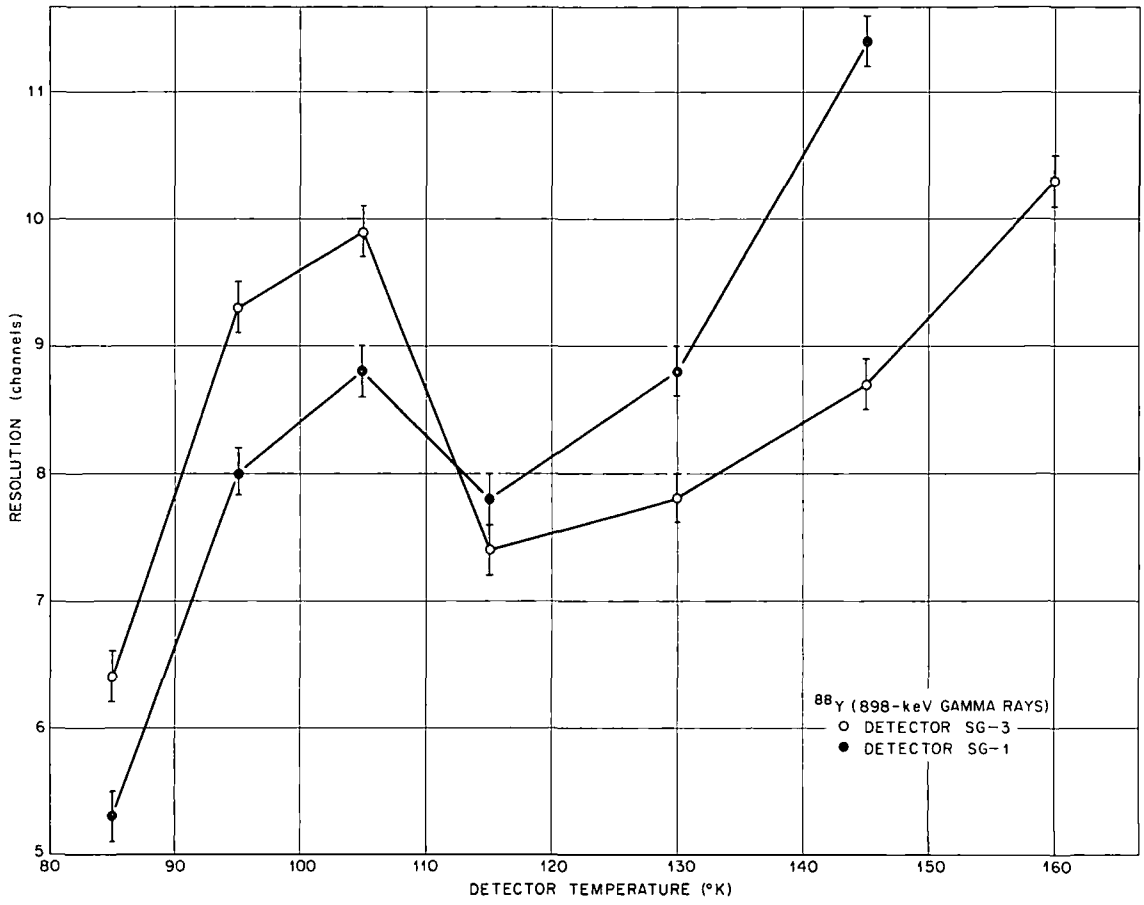

Fig. 24. Resolution of the detectors SG-3 and SG-1 on the ^{88}Y 898-kev. gamma-ray peak as function of temperature.

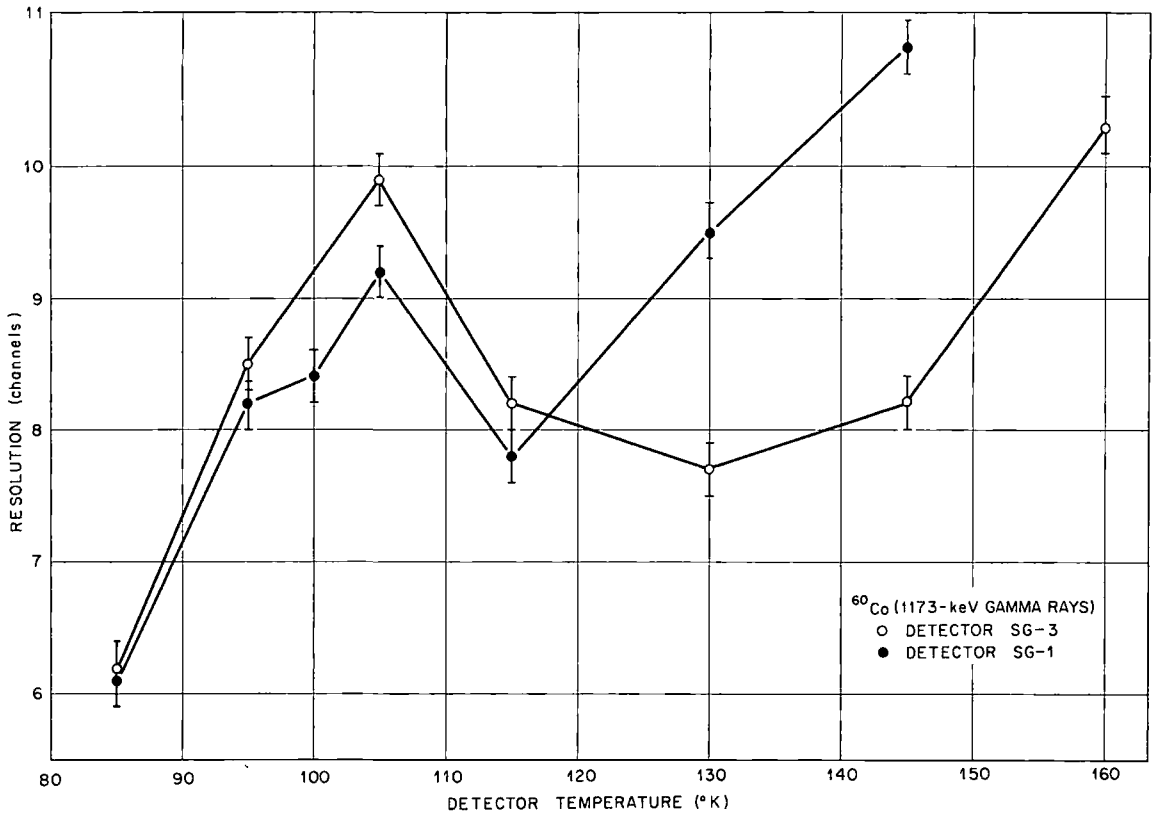

Fig. 25. Resolution of the detectors SG-3 and SG-1 on the ^{60}Co 1173-kev. gamma-ray peak as function of temperature.

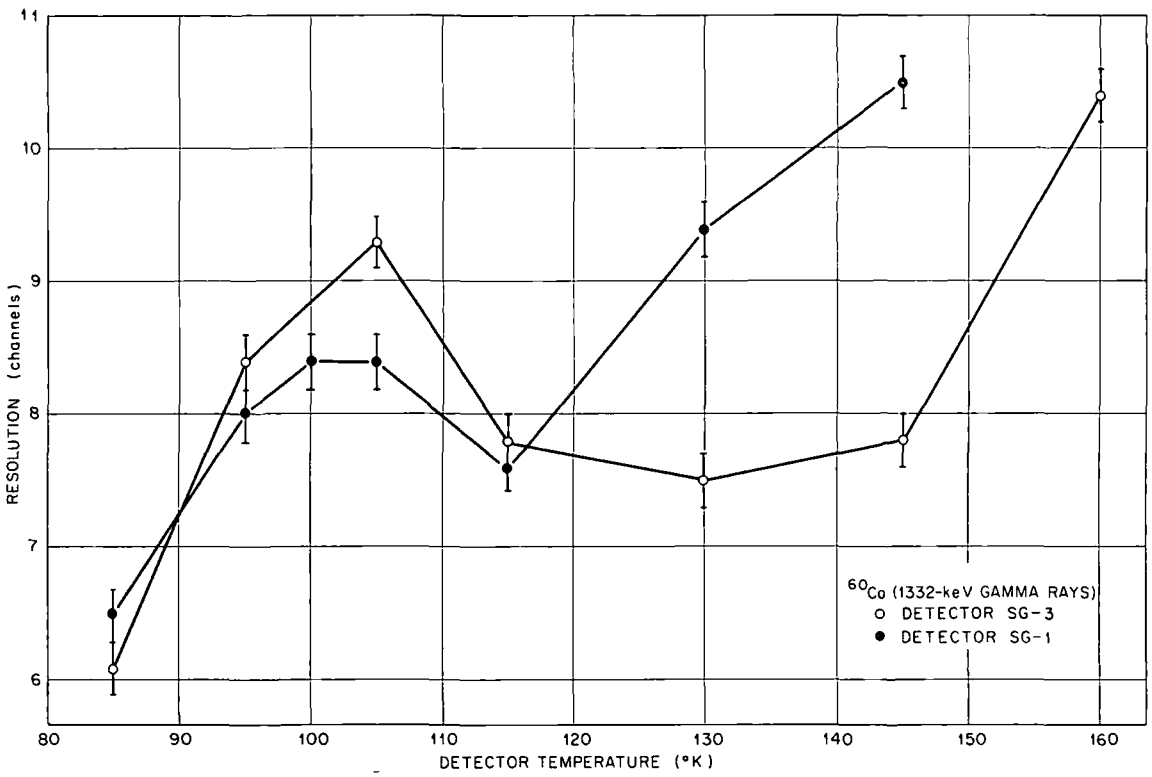

Fig. 26. Resolution of the detectors SG-3 and SG-1 on the ^{60}Co 1332-kev. gamma-ray peak as function of temperature.

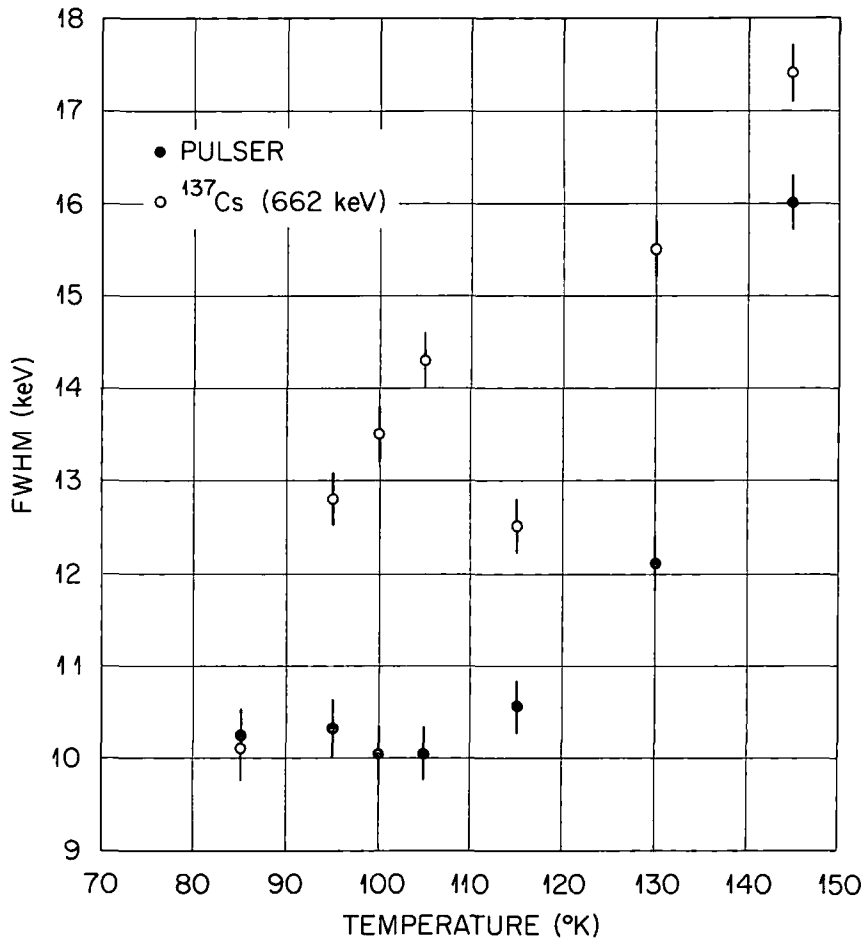

Fig. 27. Resolution of the detector SG-1 on the ^{137}Cs 662-kev. gamma-ray peak, together with pulser line width as function of temperature.

collection of the electron-hole pairs. The peaking in the resolution-temperature curve occurs only on using the gamma source, which emphasizes that this peak is a source effect.

The position of the maximum point of the gamma-ray photopeak in the pulse-height spectrum was taken as a measure of the detector pulse height. The detector pulse height for different gamma-ray energies was studied as a function of temperature and the results for both diodes SG-3 and SG-1 are shown in Figures 28, 29, 30, and 31, respectively. It is observed that as the temperature of the detector was increased, there is a very small increase in the pulse height. The amount of increase in the pulse height due to a change in temperature of 50°K. for both diodes and for different gamma-ray sources is given in Table IV.

From Table IV it is noticed that for both diodes SG-3 and SG-1 the pulse height from ^{88}Y (898-keV. gamma ray) showed the largest increase in pulse height with temperature increase.

The increase in the pulse height with temperature may be due to (1) the increase in thermal generation currents, which may add to the pulse height; (2) the reduction in the width of the band gap in germanium with increasing temperature,[19] which may reduce the energy necessary for electron hole pair formation and thus, for a given gamma ray incident on the detector at a certain temperature, will increase the detector output pulse if the detector is used at higher temperature; or (3) the trapping of the carriers before they are collected.[11,20]

The relative efficiency for the detection of the full-energy gamma peak at different temperatures is evaluated by dividing the area

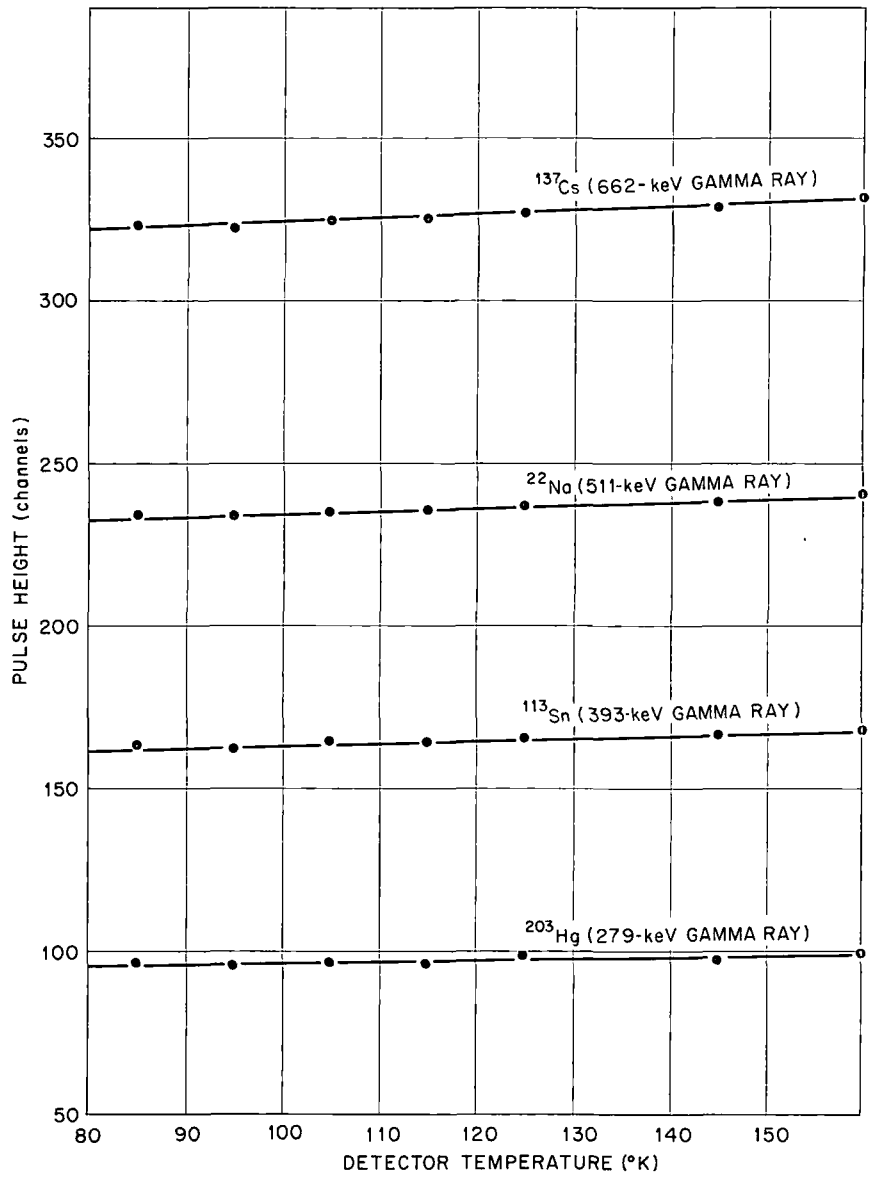

Fig. 28. Pulse heights from the detector SG-3 as a function of temperature for the lower energy gamma rays.

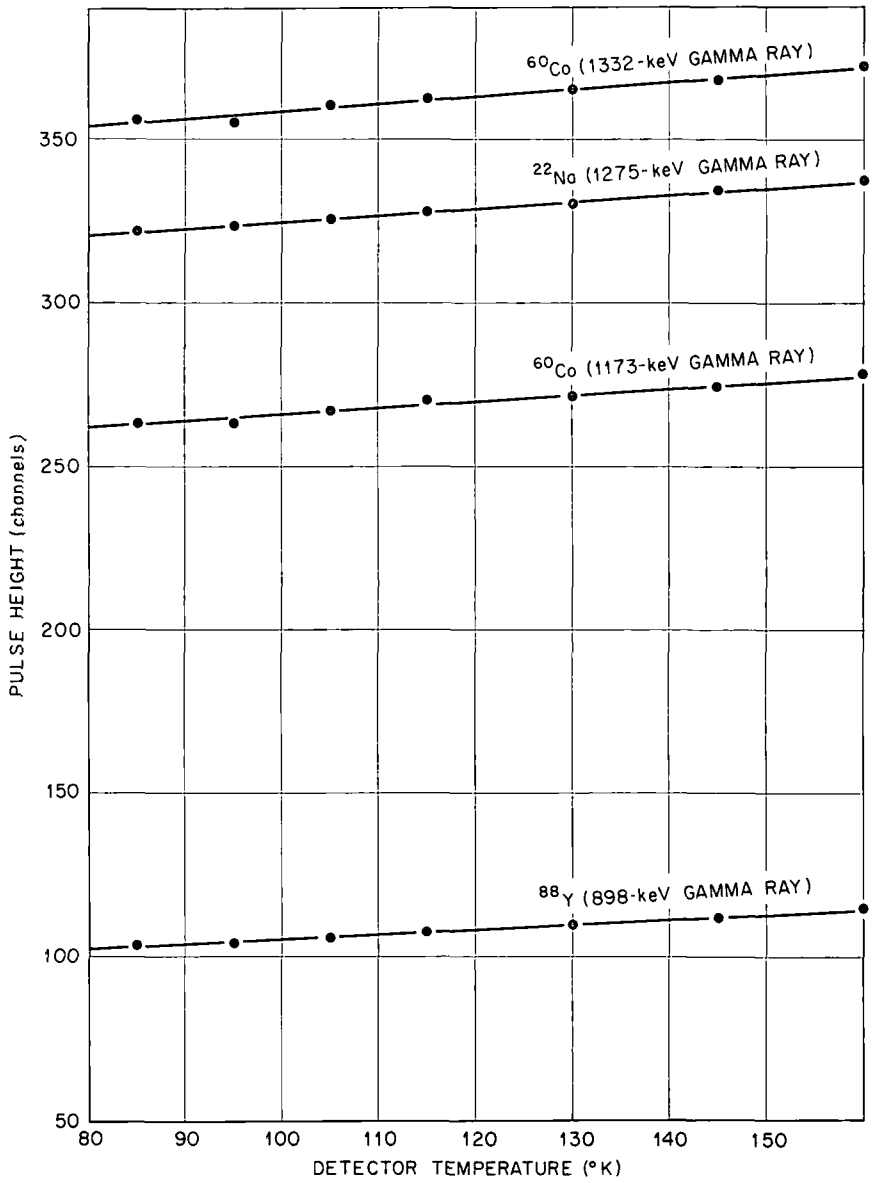

Fig. 29. Pulse heights from the detector SG-3 as a function of temperature for the upper energy gamma rays.

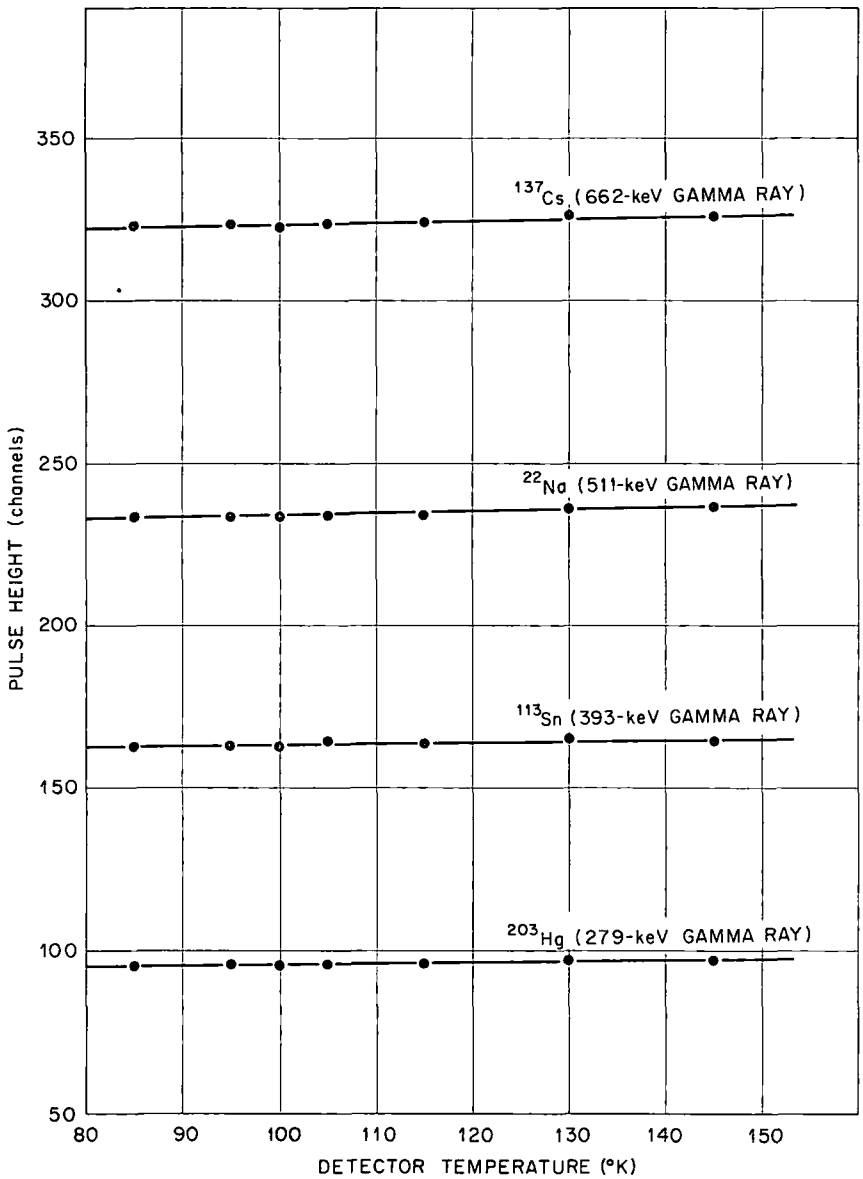

Fig. 30. Pulse heights from the detector SG-1 as a function of temperature for the lower energy gamma rays.

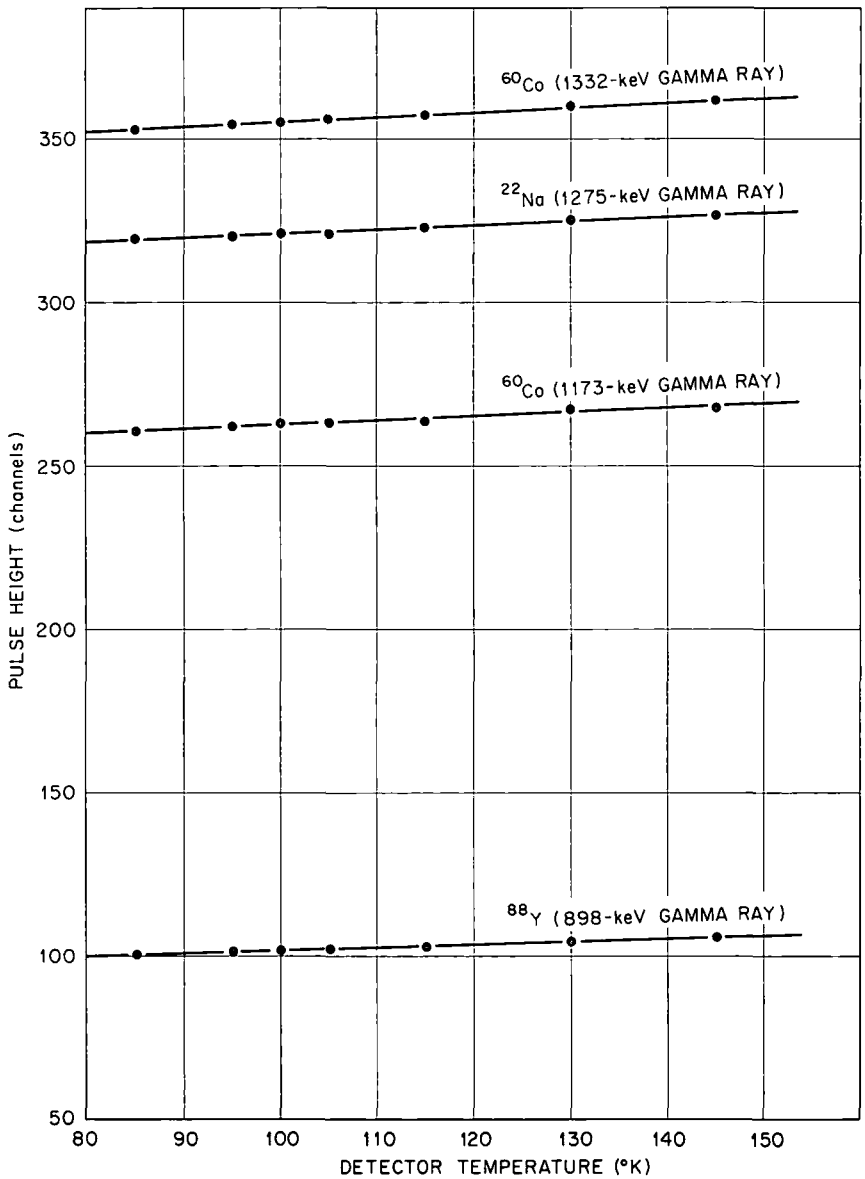

Fig. 31. Pulse heights from the detector SG-1 as a function of temperature for the upper energy gamma rays.

TABLE IV

THE PERCENTAGE INCREASE IN THE PULSE HEIGHT FOR 50°K. INCREASE IN THE DETECTOR TEMPERATURE

Source	Detector SG-1 per cent	Detector SG-3 per cent
^{203}Hg(279 keV. gamma ray)	(1.32 ± 0.54)	(2.7 ± 0.4)
^{113}Sn(393 keV. gamma ray)	(1.32 ± 0.22)	(2.23 ± 0.33)
^{22}Na(511 keV. gamma ray)	(0.88 ± 0.27)	(1.60 ± 0.21)
^{137}Cs(662 keV. gamma ray)	(0.88 ± 0.28)	(1.75 ± 0.12)
^{88}Y (898 keV. gamma ray)	(4.06 ± 0.91)	(7.5 ± 0.32)
^{60}Co(1173 keV. gamma ray)	(2.34 ± 0.16)	(3.79 ± 0.35)
^{22}Na(1275 keV. gamma ray)	(1.79 ± 0.29)	(3.26 ± 0.16)
^{60}Co(1332 keV. gamma ray)	(1.78 ± 0.13)	(3.3 ± 0.39)

under the peak by the analyzer storing time. For both diodes SG-3 and SG-1 the relative efficiencies of detecting the full-energy gamma peak with the detector at different temperatures are shown in Figures 32-37. It is found that for all gamma-ray energies the relative efficiency of the detector as function of temperature changes randomly by about ±8 per cent of the average value.

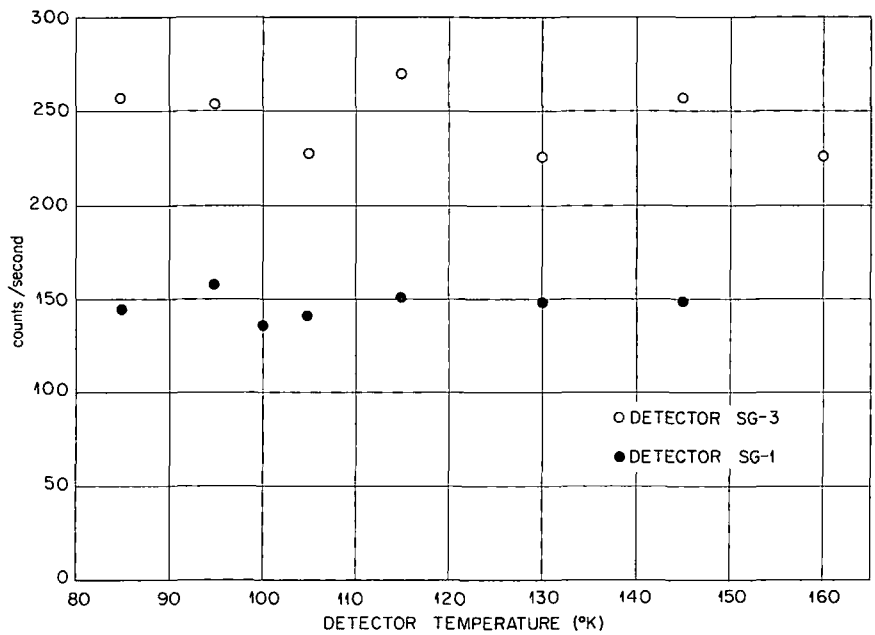

Fig. 32. The relative efficiency of the detectors SG-3 and SG-1 in detecting the ^{203}Hg 279-kev. gamma-ray peak as function of temperature.

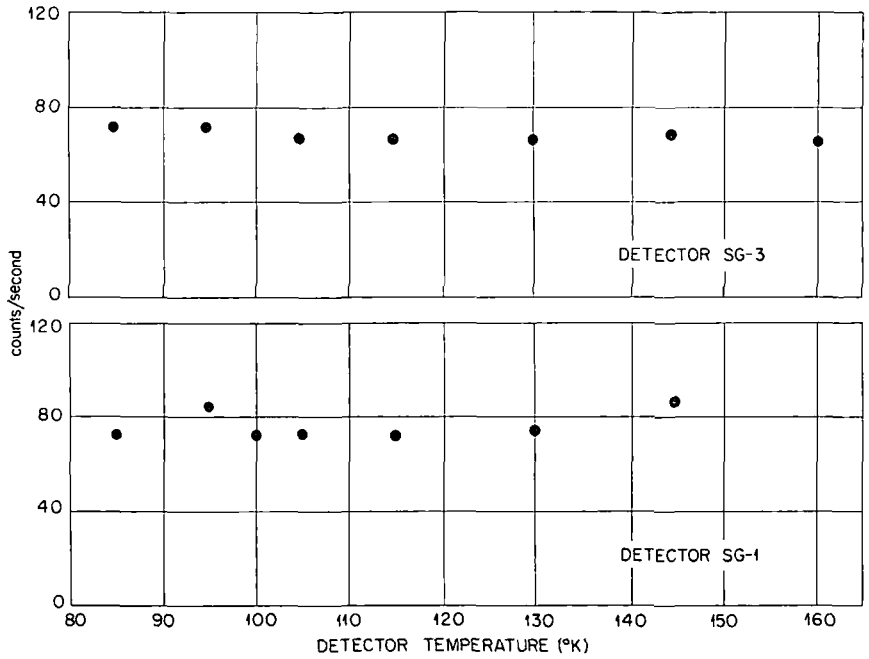

Fig. 33. The relative efficiency of the detectors SG-3 and SG-1 in detecting the ^{113}Sn 393-kev. gamma-ray peak as function of temperature.

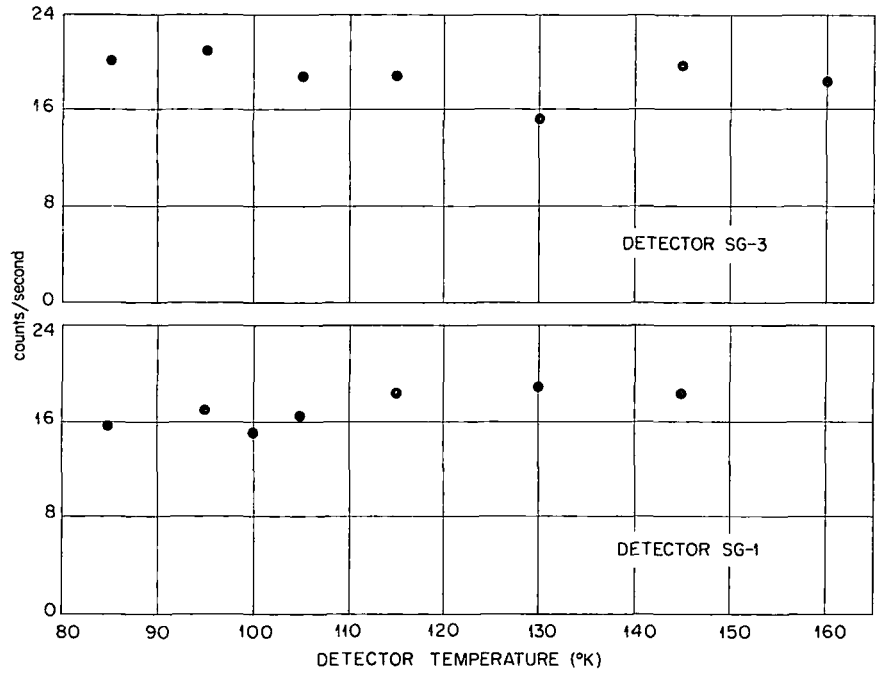

Fig. 34. The relative efficiency of the detectors SG-3 and SG-1 in detecting the ^{22}Na 511-kev. gamma-ray peak as function of temperature.

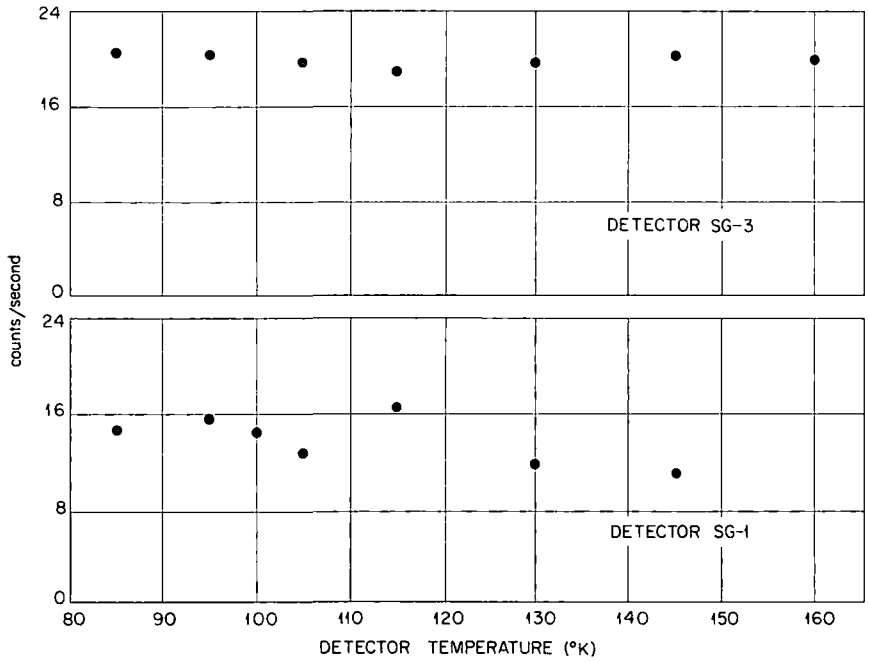

Fig. 35. The relative efficiency of the detectors SG-3 and SG-1 in detecting the ^{137}Cs 662-kev. gamma-ray peak as function of temperature.

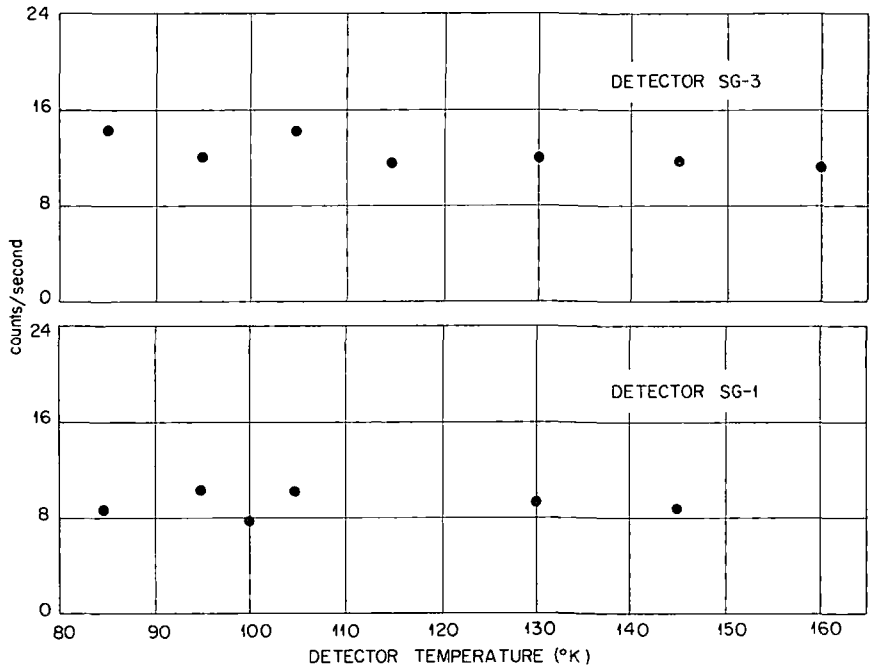

Fig. 36. The relative efficiency of the detectors SG-3 and SG-1 in detecting the ^{88}Y 898-kev. gamma-ray peak as function of temperature.

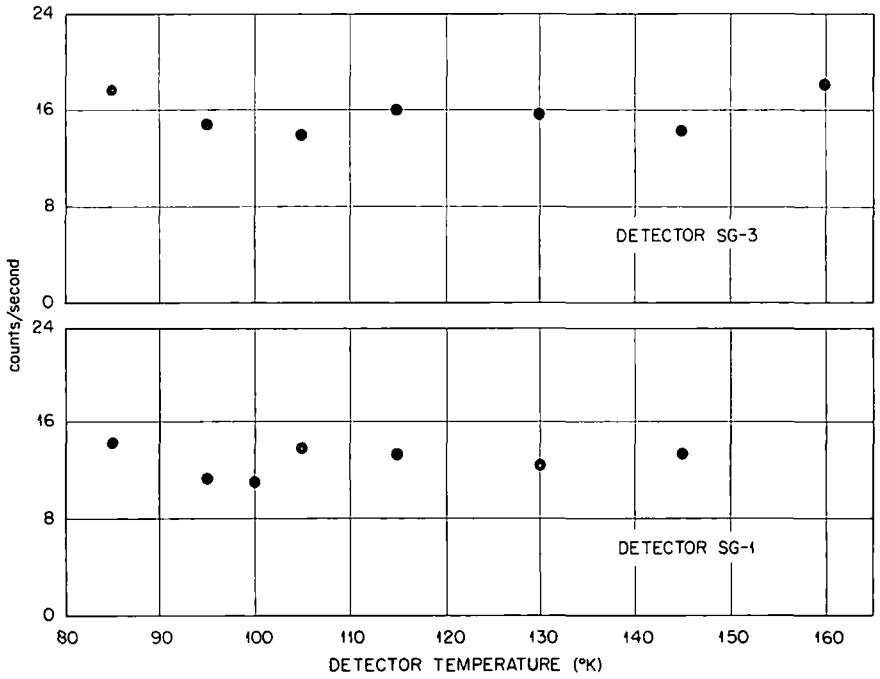

Fig. 37. The relative efficiency of the detectors SG-3 and SG-1 in detecting the ^{22}Na 1275-kev. gamma-ray peak as function of temperature.

CHAPTER V

CONCLUSION

The two lithium-drifted germanium detectors SG-3 and SG-1 showed a peak in the resolution versus temperature curve at about 105°K. This is contrary to the results of Tavendale[10] who did not observe such a peaking when he studied the resolution for a germanium detector (diameter = 19 mm., width = 3.5 mm.) on the ^{57}Co 122-keV. gamma-ray peak as a function of temperature.

Measurements of the leakage current, the capacitance, and the resolution using the mercury pulser for both diodes, together with the resolution as function of bias voltages for diode SG-1 at 85° and 105°K., emphasize the fact that this peaking in the resolution is an effect that appears on using a gamma-ray source. Since the two diodes were cut from the same germanium ingot, it is possible that these results are peculiar to these two detectors. Repeating the experiment on different diodes (cut from different germanium ingots), with particular care in the temperature range where this peak appeared, will prove whether this peaking in the resolution is or is not a characteristic of lithium-drifted germanium gamma-ray detectors.

If the repeated measurements with different diodes show that such a peaking in the resolution is peculiar to the two diodes SG-3 and SG-1, one would suspect possible diffusion of "unwanted" impurities inside the germanium crystal during the lithium-drifting process which may change the detector properties.

1. E. M. Pell, J. Appl. Phys. 31, 291 (1960).

2. E. M. Pell, Natl. Acad. Sci. Publ. 871, 136 (1961).

3. D. V. Freck and J. Wakefield, Nature 193, 669 (1962).

4. P. P. Webb and R. L. Williams, Nucl. Instr. and Methods 22, 361 (1963).

5. A. J. Tavendale, Electronique Nucleaire, 1963 (O.E.C.D., Paris), p. 235.

6. A. J. Tavendale and G. T. Ewan, Nucl. Instr. and Methods 25, 185 (1963).

7. A. J. Tavendale and G. T. Ewan, Bull. Am. Phys. Soc. 9, 47 (1964).

8. G. T. Ewan, Bull. Am. Phys. Soc. 9, 8 (1964).

9. G. T. Ewan and A. J. Tavendale, Nucl. Instr. and Methods 26, 183 (1964).

10. A. J. Tavendale, IEEE Trans. Nucl. Sci. NS-12, 255 (1965).

11. G. T. Ewan and A. J. Tavendale, Can. J. Phys. 42, 2286 (1964).

12. H. L. Malm, A. J. Tavendale, and I. L. Fowler, Can. J. Phys. 43, 1173 (1965).

13. J. M. McKenzie and D. A. Bromley, Phys. Rev. Letters 2, 303 (1959).

14. J. M. McKenzie and D. A. Bromley, Bull. Am. Phys. Soc. 4, 422 (1959).

15. J. L. Blankenship and C. J. Borkowski, IRE Trans. on Nucl. Sci. NS-8(1), 17 (1961).

16. "Low Noise Amplifier for Use with Solid State Detectors," Oak Ridge National Laboratory, TID-6119 (1960).

17. R. L. Powell et al., "Low Temperature Thermocouples," Temperature: Its Measurement and Control in Science and Industry, Vol. 3 (New York, Reinhold Publishing Corporation, 1962), p. 65.

18. F. S. Goulding, Nucleonics 22, 54 (1964).

19. N. B. Hannay (ed.), Semiconductors, No. 140 (New York, Reinhold Publishing Corporation, 1959).

20. D. C. Northrop and O. Simpson, Proc. Phys. Soc. 80, 262 (1962).

Internal Distribution

1-2. L. S. Abbott
3. R. G. Alsmiller, Jr.
4. F. E. Bertrand
5. W. R. Burrus
6. V. R. Cain
7. G. T. Chapman
8. C. E. Clifford
9. W. A. Gibson
10. N. Hill
11. L. B. Holland
12. T. A. Love
13. F. C. Maienschein
14. F. J. Muckenthaler
15. R. W. Peelle
16. S. K. Penny
17. J. C. Pigg
18. R. T. Santoro
19. H. A. Todd
20. J. H. Todd
21. V. V. Verbinski
22. J. W. Wachter
23-62. W. Zobel
63. G. Dessauer (consultant)
64. B. C. Diven (consultant)
65. M. L. Goldberger (consultant)
66. M. H. Kalos (consultant)
67. L. V. Spencer (consultant)
68-69. Central Research Library
70. Document Reference Section
71-252. Laboratory Records
253. Laboratory Records ORNL RC
254. ORNL Patent Office

External Distribution

255-269. Division of Technical Information Extension (DTIE)
270. Research and Development Division (ORO)